Estimating Specific Leaf Area (SLA) in saltmarsh/ wetland ecosystem, using Sentinel-2 data, a case study of Schiermonnikoog island
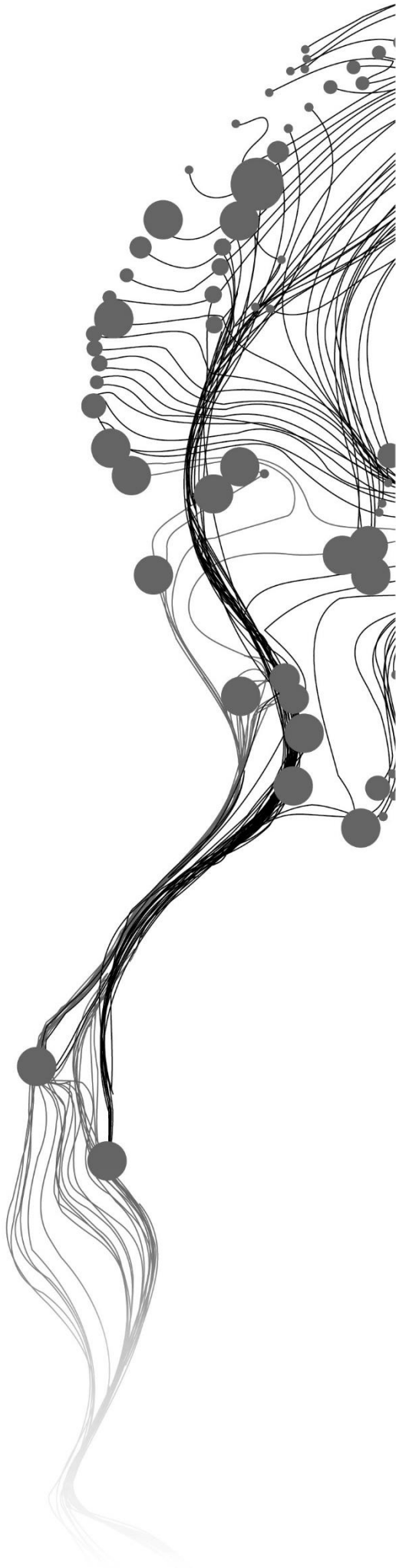
KASRA RAFIEZADEH SHAHI
March 19, 2018

SUPERVISORS:
Dr.R.Darvishzadeh
Prof.dr.A.K.Skidmore

Estimating Specific Leaf Area (SLA) in saltmarsh/wetland ecosystem using Sentinel-2 data, a case study of Schiermonnikoog island

KASRA RAFIEZADEH SHAHI
Enschede, The Netherlands, March 19, 2018

Thesis submitted to the Faculty of Geo-Information Science and Earth Observation of the University of Twente in partial fulfilment of the requirements for the degree of Master of Science in Geo-information Science and Earth Observation.
Specialization: [Natural Resource Management]

SUPERVISORS:
Dr.R.Darvishzadeh
Prof.dr.A.K.Skidmore

THESIS ASSESSMENT BOARD:
Dr.ir.C.A.J.M. de Bie (Chair)
Dr, M, Azong Cho (External Examiner, Council for Scientific and Industrial Research (CSIR))

ABSTRACT

Specific Leaf Area (SLA) is one of the proposed Essential Biodiversity Variables (EBVs) to monitor biodiversity changes. In addition, SLA has a strong correlation with photosynthesis capacity and nitrogen content and therefore, it is an appropriate indicator to monitor plant functional process (e.g. plant growth, plant productivity). Regarding to time and expense, traditional survey methods are not appropriate approaches to monitor biodiversity changes; but Remote Sensing (RS) data is a non-destructive and efficient manner to obtain information on biodiversity changes. Among the new satellites, Sentinel-2 satellites which were launched recently provide high spatial, temporal, and spectral resolution imageries.

Further, statistical approaches as follow have been examined to estimate SLA: 1) Univariate models (Vegetation Indices (VIs)), and 2) Multivariate models (Artificial Neural Network (ANN), Partial Least Square Regression (PLSR)). The selected multivariate models (ANN, and PLSR) to our knowledge have not been used to estimate SLA. Therefore, the usability of Sentinel-2 data and the performance of different statistical approaches have been studied in saltmarsh/ wetland ecosystem.

Field data were collected in Sciermonnikoog island from 26th September to 5th October, and a number of plant parameters including Leaf Area (LA) and Leaf Dry Mass Content (LDMC) were measured for 50 sample plots. The Sentinel-2 image was downloaded on 15th September 2017, and the correlation between the measured SLA and Sentinel-2 spectral data were examined. In this study, 9 individual bands (20 meters spatial resolution) of Sentinel-2 data and 11 VIs have been used to estimate SLA.

The results showed that there was a weak correlation between the measured SLA and LA (R=0.17); while, there was a strong negative correlation between measured SLA and LMDC (R=-0.73). After that, the correlation analysis between VIs with the measured SLA showed the strongest correlation is between the Ratio Vegetation Index and the measured SLA. Therefore, RVI was used to estimate SLA through different regression techniques (simple linear, quadratic, logarithmic, exponential regression). The findings illustrated that SLA could be estimated by RVI using simple linear regression (R^2=0.46, RMSE=0.64).

Among the studied multivariate models (ANN, and PLSR) the performance of the ANN model (R^2=0.55, RMSE=0.47) which used all 11 studied VIs as input, and Levenberg-Marquardt training algorithm obtained more accurate results to estimate SLA compared to PLSR. The reason of the higher accurate performance of ANN might be the non-linear relation between explanatory variables and the response variable. However, the non-linear relation between measured SLA and predicted SLA by the ANN model might be caused by the situation on the field as follow: 1) High percentage of dead materials 2) Background material that influenced the spectral reflectance information. Moreover, 3) The possible errors that happened during plant parameters measurement.

Therefore, regarding results of the present study we conclude that: 1) SLA can be estimated accurately using Sentinel-2 data, 2) SLA could be estimated accurately through RVI (using simple linear regression) 3) SLA could be estimated accurately via ANN. In addition, some recommendations for further studies have been suggested as follow: 1) Using different multivariate approaches such as Support Vector Machine (SVM) and Random Forest (RF) to estimate SLA in saltmarsh/ wetland ecosystem, 2) Using accurate equipment to measure plant parameters, and 3) A higher number of samples is recommended as well.

Keywords: Specific Leaf Area, Sentinel-2, Schiermonnikoog, saltmarsh/ wetland ecosystem, univariate models, multivariate models.

ACKNOWLEDGEMENTS

TABLE OF CONTENTS

LIST OF FIGURES

LIST OF TABLES

ABBREVIATIONS

RS: Remote Sensing

VIs: Vegetation Indices

SLA: Specific Leaf Area

LA: Leaf Area

LDMC: Leaf Dry Matter Content

ANN: Artificial Neural Network

PLSR: Partial Least Square Regression

CV: Coefficient of Variation

1. INTRODUCTION

In this chapter, the importance of Specific Leaf Area (SLA) and RS data elaborated, and the relevant literature on this topic has been reviewed. At the end of this chapter, the research problem stated, and research questions and research hypothesis were formulated.

1.1. Background

1.1.1. Importance of SLA

In biodiversity studies, biological diversity covers a broad concept of all spatial and temporal variation of an ecosystem that corresponded to each species, their structures, and their functions (Tilman, 2001). Functional diversity is a subset of this broad concept, that describes elements (traits) of biodiversity. Functional diversity is important to realize how an ecosystem operates and it directly or indirectly influences the ecosystem processes such as productivity, resource dynamics, and other aspects of ecosystem processes (Tilman, 2001).

In plants, a trait is defined as a physiological, morphological, or phenological property that can be measured (Violle et al., 2007). Moreover, a trait can be referred as a functional trait when the trait influences on plant functions such as plant height, nutrient acquisition, and retention resources strategies (Lavorel et al., 2011). Therefore, quantifying values and ranges of functional traits will help us to understand the ecosystem functioning and to manage and make future scenarios (Homolová et al., 2013a; Lavorel et al., 2011; Tilman, 2001).

As Pereira et al., (2013) reported that decreasing biodiversity loss and preventing biodiversity changes are main international goals that shall be met till 2020; thus, some biodiversity variables were identified as Essential Biodiversity Variables (EBVs) to track biodiversity changes. However, there are still ongoing projects to find EBVs to monitor biodiversity. One of the EBVs that suggested by Skidmore et al., (2015)to capture biodiversity changes from space is Specific Leaf Area (SLA). It is also known as specific leaf mass, or leaf specific mass (Ali et al., 2016a). SLA is the ratio of the leaf area to leaf dry mass and is usually expressed in the following unit (m²/kg).

SLA can be a good indicator to describe the relationship between nutrient supply and water availability with the atmospheric CO_2 uptake (Pierce et al., 1994). In addition, SLA has a straight relationship with photosynthetic capacity (Reich et al., 1998); furthermore, photosynthetic capacity is strongly correlated with leaf nitrogen content (Evans, 1989); therefore, SLA can be a good indicator to address plant growth and plant production (Hikosaka, 2004). Generally, different species have different SLA (Poorter and Jong, 1999); for instance, high-SLA species have high concentrations of nitrogen and high rates of CO_2 which is indicating the species have a high rate of photosynthesis process; in contrast, low-SLA species have high concentrations of cell walls and also this type of species have greater leaf and root longevity (Poorter and Jong, 1999).

1.1.2. Importance of Remote Sensing in monitoring SLA

As it is mentioned in Section 1.1.1, monitoring SLA in large-scales is important to provide valuable information about plant growth, photosynthesis capacity, and other aspects of plant physiological processes (Ali, 2016; Pierce et al., 1994). However, SLA estimation is a challenging task at regional and global scales yet (Pierce et al. 1994). In addition, to monitor this plant functional trait at large- scales, traditional surveying methods are not efficient regard to temporal and financial perspectives (Duro et al., 2007). Thus, an alternative way to monitor SLA is needed.

Remote sensing is a non-destructive and cost-efficient way to collect data about different biodiversity variables at large-scales compared to traditional manners (De Roeck et al., 2008; Song et al., 2013). In the past decades, satellites data such as Landsat TM, or SPOT have been frequently used to study vegetation covers and their characteristics. Nonetheless, recently, the use of the new generation satellites has been increasing to measure and estimate biophysical and biochemical parameters (Adam et al., 2010; Ali et al., 2017a). Remote sensing is an appropriate alternative to traditional survey for tracking and monitoring biodiversity variables; since, biodiversity variables contain different kinds of spectral, spatial, and temporal information.

The data of the newly launched satellites have spatially, spectrally, and temporally improved. By this new generation of satellite technologies, many biodiversity variables can be monitored, and biological issues can be solved. Among them, Sentinel-2 is one of the newly launched high spatial resolution satellite that is equipped with the multispectral instrument. Sentinel-2 provides data continuity and enhancement of Landsat and SPOT data (Wang et al., 2017). Although, Sentinel-2 data has been using to estimate the number of biophysical and biochemical parameters (Clevers et al., 2017; Korhonen et al., 2017), to our knowledge, the Sentinel-2 data still is not explored for SLA estimation.

In addition, to the importance of RS data, it is a crucial issue to find precise and robust retrieval methods for biophysical parameters (Verrelst et al., 2012). There are different kinds of methods for vegetation parameters retrieval that will be discussed in the next Section.

1.1.3. Analytical approaches to estimate SLA by using RS data

A model is an abstraction of the real world which means models, help us to realize how different systems around us are working (Rogers, 2012). There are different models that can be used to estimate plant variables from RS data. Among them, two different modelling approaches are mostly used; they are namely statistical and physical models (Skidmore, 2002).

Statistical models widely used to make a statistical relationship between the measured vegetation parameter *in situ*, and the spectral reflectance derivatives at a specific wavelength or from a combination of wavelengths(e.g. Vegetation Indices) (Homolová et al., 2013b). Statistical models, based on their processing methods and logic could be categorized as deterministic and inductive models (Skidmore, 2002); in addition, they can be divided into the two following categories: 1) Univariate models (Schowengerdt, 2012) (e.g. Vegetation Indices), 2) Multivariate models (Chang, 2000; Curran et al., 2001; Wold et al., 2001) (e.g. neural networks, simple multiple linear regression, partial least square) .

In the first category, there is a one to one relationship which means the parameter of interest only can be modelled by one explanatory variable. The explanatory variable can be spectral reflectance of an individual band or an index calculated by spectral reflectance of different bands (e.g. NDVI, or EVI) of the satellite imageries (Lymburner et al., 2000). In the second category, it is a one to many relationships that means the vegetation parameter can be modelled by several independent variables (such as a combination of several bands). A number of biophysical parameters have been studied using multivariate models (Hansen and Schjoerring, 2003; W. Li et al., 2016), however, only limited studies exist on SLA estimation using these models (Ali et al., 2017a; Lymburner et al., 2000).

Another modelling approach is physical models also known as Radiative Transfer Models (RTMs). They are used to derive a number of plant functional traits, although, to retrieve vegetation parameters, RTMs should be inverted (Goel and Strebel, 1983).The choice of the RTMs and the inversion strategy are important factors for successful retrieval of plant traits (Atzberger et al. 2013). Nevertheless, utilization RTMs are expensive and faced with an ill-posed problem (which result when different combinations of model parameters produce almost identical spectral reflectance (Quan et al., 2015)). There are many studies that have been conducted for estimating vegetation parameters using physical models (Ali et al., 2016c; Darvishzadeh et al., 2011, 2008; Myneni, 1997).

1.2.   Literature review

Remote Sensing (RS) data are the most common data type that has been used for biodiversity studies. For instance, Sánchez-Azofeifa et al., (2009) used RS data to differentiate leaf properties (such as SLA) and spectral properties of liana and tree communities from a tropical dry forest and a tropical rainforest in Panam, Central America. According to Sánchez-Azofeifa et al., (2009)'s results, the leaf properties and spectral properties of both liana and tree communities were different in a tropical dry forest; nevertheless, in a tropical rainforest, the indicated properties are not different. In addition, among the leaf properties, SLA was significantly higher for liana leaves compared to tree leaves; in other words, tree communities conserve resources; nonetheless, lianas had higher resources and consumptions. In another study Asner et al., (2008) investigated on discriminataion between native and invasive species in Hawaiian forests; they used spectral data acquired from Airborne Visible and Infrared Imaging Spectrometer (AVIRIS), and then linked them to leaf properties (e.g. SLA, leaf nutrients). They showed that, using spectral and leaf properties together makes the possiblility to discrimantie between native, and invasive species in Hawaiian forest. Moreover, as it is described by Ali et al., (2016b), among different functional traits, SLA and leaf dry matter content are important leaf properties to measure biodiversity.

According to several studies (Darvishzadeh, 2008a; Liang, 2004; Schowengerdt, 2012), there are different data models that have been using to analyse and to process RS data, which the most common used data models in RS subjects are univariate and multivariate models.

1.2.1.   Statistical approaches

1.2.1.1.   Univariate models

Schowengerdt, (2012), defined univariate models as a single band image that can be used through mathematical models to apply for image processing. Univariate approaches based on Vegetation Indices (VIs) have been studied in several types of research to estimate vegetation parameters (Amiri et al., 2010; Du Plessis, 1999; Haboudane et al., 2004; Paruelo and Tomasel, 1997). For instance, Darvishzadeh et al., (2009) studied the comparison between different narrow-bands VIs to estimate LAI; furthermore, it is illustrated to estimate vegetation parameters, mostly VIs that are calculated from near-infrared and red spectral regions. The reason why these ranges of spectral reflectance are appropriate to estimate vegetation parameters is that they are highly corelated to chlorophyll and biomass abundance. However, there are only a few studies that have investigated on the SLA estimation using multispectral imageries through calculating VIs (Ali et al., 2017c; Lymburner et al., 2000).

Lymburner et al., (2000) investigated the correlation of individual bands and different VIs with SLA using multispectral Landsat TM imageries in Ku-ring-gai Chase National Park on Lambert Peninsula, Australia and found that there is strong correlation between SLA and the following VIs: 1) Soil and Atmospheric Resistant Vegetation Index(SARVI), 2) Normalized Difference Vegetation Index(NDVI), 3)Ratio Vegetation Index (RVI).Moreover, Ali et al., (2017a) investigated on SLA estimation based on statistical and physical approaches using Landsat 8 in the mixed mountain forest of Bavarian National Park, Germany and demonstrated that there is a strong linear relationship between SLA and Enhanced Vegetation Index(EVI).

1.2.1.2.   Multivariate models

In contrast, as Schowengerdt, (2012) defined, multivariate models, can use a multi-band image or a combination of band images to process images. In several studies, multivariate approaches have been used to estimate a number of vegetation parameters such as water content and LAI from RS data (Darvishzadeh, 2008; Fang & Liang, 2003). The multivariate approaches such as Artificial Neural Network (ANN), and Partial Least Square Regression (PLSR), are used to reduce the multicollinearity, which is a common problem when a high number of explanatory variables exist (Mirzaie et al., 2014). Nevertheless, these algorithms have been rarely used to estimate SLA. Therefore, retrieval of SLA using these approaches needs further investigations.

The idea of ANN algorithm is to make a model that to process data approximately like the human brain but with less complexity (Kohonen, 1988). The reason of applying ANN is that the human brain is able to process a huge amount of data obtained from different sources; in human brain neural-elements known as neurons will receive inputs, and after processing, neurons will produce an output (Atkinson and Tatnall, 1997).

ANN fundamentals has been investigated by Mcculloch and Pitts, (1990), which described the complete structure of a neural network and its elements. Moreover, later on, this technique has been used for different applications such as pattern recognition (Messier, 1991), decision making (Messier, 1991), robot control (Husbands et al., 1998) as well. As it is mentioned above, this technique can be applied to process vast quantities of dataset; therefore, researchers investigated on the efficiency of utilization ANN for remotely sense dataset (Benediktsson et al., 1993; Chen et al., 1997; Serpico et al., 1996; Tiwari et al., 1999).

ANN is a non-parametric algorithm that has been used in many different environmental applications such as estimation of soil properties, and estimation of vegetation biophysical parameters (Bacour et al., 2006; Chang, 2000; Fang and Liang, 2003). The main parts of each ANN model are inputs, hidden layers, output(s); that generally depend on the objectives of studies these parameters can be different. In biodiversity studies which focus on estimation of biophysical parameters with ANN models through RS data, mostly ANN models include a number of inputs used from RS data and one output which is the interested biophysical parameter in the study (Atzberger, 2004; P. Liu et al., 2017; Paruelo and Tomasel, 1997; Ushada and Murase, 2006).

In hidden layers, there are some connected neurons and activation functions (Mirzaie et al., 2014). There are different ANN algorithms. One of the ANN algorithm is multi-layer perceptron which can model non-linear functions and can be accurately generalized to an independent dataset (Gardner and Dorling, 1998). Moreover, multi-layer perceptron makes no initial priority between inputs based on the data distribution (Hornik et al., 1989). The structure of multi-layer perceptron as explained earlier include inputs, hidden layers, and outputs; however, using suitable weights and transfer functions between neurons helps the ANN model to accurately estimate the output (Gardner and Dorling, 1998). Therefore, training the multi-layer perceptron network is an essence to modify the weights and transfer functions. Among the different training algorithms, back-propagation algorithm is most popular training algorithm to train the multi-layer perceptron (Rumelhart et al., 1985); the back-propagation algorithm consists of two different processes forward and backward propagation. In backward propagation process, the training algorithm modifies the weights between neurons from output to input; this process results in decreasing error of the model. On the other hand, in forward propagation process, the modifying process of neuron's weight start from the input to output layer (Atkinson and Tatnall, 1997).

Therefore, the training algorithm to train the network play an important role as well as selecting the number of neurons that are important in the performance of the network (Riedmiller and Braun, 1993). Although the backpropagation algorithm is easy to implement, this algorithm converges slowly; even it is also possible that the backpropagation algorithm does not converge (Jiao et al., 2001). As it is defined in most artificial neural network studies, convergence means " a set of weights along the supervised training of an ANN model which used to find (converge on) needed values for producing trained response" (Glossary of Neural Network Terms, 2018).

Several training algorithms have been proposed to cope the convergence problem in backpropagation algorithm. For instance, one of the proposed algorithm by Riedmiller and Braun, (1993), is resilience backpropagation that established to make the process faster and more efficient than the traditional backpropagation. According to Demuth et al., (2017), another training algorithm is Levenberg-Marquardt (trainLM) that is one of the fastest training function in general; in addition, the efficiency of this algorithm is for smaller networks because trainLM does not need a huge memory and computation time. Furthermore, trainLM has better performance in function fitting (non-linear regression) problems. One more training algorithm that has been used mostly in large networks is Scaled Conjugate Gradient (trainSCG), one of the advantages of trainSCG is that this algorithm does not need a high amount of memory.

The Partial Least Square Regression (PLSR) was developed by Wold in the late 1960s to use it for economical purposes (Wold, 1975) but utilizing PLSR method in ecological applications started in the late 1990s. However, using PLSR method in ecological applications based on the RS data have been increased in the last years; for instance, this method has been used to predict biophysical and biochemical parameters (Hansen and Schjoerring, 2003; Mirzaie et al., 2014; Siegmann and Jarmer, 2015; Wolter et al., 2009) and crop yield (Foster et al., 2017; Ye et al., 2008).

PLSR is a bilinear regression technique to decrease a large number of predictor variables to a few numbers of non-correlated predictor variables, then using the non-correlated variables to predict the response variable (Hansen and Schjoerring, 2003). As Carrascal et al., (2009) reported, in PLSR model, the correlation between response variable and different combination of predictor variables are analysed in order to find the non-collinear predictor variables. The relation between predictor variables and the response variable are made by latent factors which maximize the explained variance of predictor variables in the response variable. PLSR model uses the relationship between predictor variables and the response variable to decrease the number of factors to a lower number efficient factors. These efficient factors help the model to make an accurate relationship between the response variable and predictor variables (Geladi and Kowalski, 1986; Hubert and Vanden Branden, 2003; Tobias, 2003).

The main reasons for using PLSR models are as follow (Stone, 1974; Wolter et al., 2009): 1) When there is a strong correlation between predictor variables (Multicollinearity problem), 2) When the number of predictor variables are higher or the same as the number of collected data (Overfitting) which also makes difficulties to calculate coefficient of determination of the PLSR model.

1.3. Research problems

As was highlighted in Section 1.1.3, although SLA has an important role in explaining photosynthesis capacity, nitrogen content, and generally in biodiversity, there are only limited studies that have been performed to estimate SLA using remotely sensed data. While these studies have been mostly conducted in forest ecosystems (Ali et al., 2017c, 2016c; Lymburner et al., 2000). Furthermore, the most studies (Ali et al., 2016d; Asner et al., 2009; Ball et al., 2015a; Klem et al., 2012; Van Wittenberghe et al., 2014) estimated SLA through hyperspectral data which are expensive and are not always available.

Therefore, an appropriate alternative will be using multispectral RS data to estimate SLA. As was indicated in Section 1.1.2, the new generation of satellites carry on the state-of-the-art technologies to capture data, that make a great opportunity to monitor biodiversity variables repeatedly with high spatial and temporal resolutions. Among the recently launched satellites, Sentinel-2 with the systematic acquisition of high-resolution multispectral data has rarely been used for SLA estimation.

In addition, as was mentioned in Section 1.2, multivariate methods ANN, and PLSR; although have been studied to estimate and retrieve a number of vegetation parameters (Banskota, 2006; Fang et al., 2014; Grace, 2017; Verrelst et al., 2012), they have been rarely examined for SLA retrieval in a saltmarsh/ wetland ecosystem. Therefore, in this study by implementing different statistical approaches using Sentinel-2 data; robust and accurate empirical models to estimate SLA in saltmarsh will be identified.

1.4. Research Objectives

The main aim of this study is *to model SLA by different statistical models in a saltmarsh/wetland ecosystem area using Sentinel-2 data.*

The specific objectives of this study are as follow:

- To model SLA using Vegetation Indices (VIs) calculated from Sentinel-2 data.

- To model SLA using Artificial Neural Networks (ANN) and Partial Least Square Regression (PLSR) from Sentinel-2 data.

1.5. Research questions

Following research questions will be answered in this study.

1) Among the studied VIs, which index will more accurately (Highest R^2 and lowest RMSE) model SLA in Schiermonnikoog using Sentinel-2 data?

2) Among the studied multivariate models (ANN, PLSR), which model will accurately model SLA in Schiermonnikoog using Sentinel-2 data?

1.6. Research hypothesis

The research hypotheses are as indicated below:

1) Among the studied VIs, the Ratio Vegetation Index (RVI), will model the SLA more accurately (In terms of R^2 and RMSE).

2) ANN will model SLA more accurately (Higher R^2 and lower RMSE) compared to PLSR.

1.7. Expected outputs

Following the research objectives, questions and hypotheses, we anticipate obtaining the following outputs:

1) Several vegetation indices, including RVI will be examined to model SLA, in Schiermonnikoog, using ground truth measurements and Sentinel-2 data.

2) Multivariate models, including ANN, and PLSR calibrated for estimating SLA using ground truth measurements and Sentinel-2 data in Schiermonnikoog.

2. STUDY AREA AND DATA

2.1. Study area

Schiermonnikoog is one of Dutch barrier islands which is located in the northern part of the Netherlands (Province of Friesland) with 53° 29' 21.7464" N, 6° 13' 51.2796" Geographical coordinates (Figure **2.1**). The area of the island is about 40 km^2 and the island contains one village with approximately 1000 inhabitants (Mulatu, 2006). A yearly rainfall and temperature are 10.2℃ ± 0.72℃ (mean ± SD) and 824mm ± 149.1mm respectively ("KNMI," 2018; Schrama, 2012). The greater part of the island is allocated to natural landscapes including beach which is located in the northern part of the island, dune which is extended from west to east of the island, and saltmarsh which is located in the south and southeastern part of the island (Schmidt et al., 2004; Vrieling et al., 2017). Moreover, the island met the wetlands criteria and was designated as a Ramsar Site in 2014 (the Secretariat of the Ramsar Convention, 2015). Therefore, the island is also considered as a valuable coastal wetland site for essential ecological services which are needed to maintain and improve the health of the environment (Mulatu, 2006).

The vegetation cover of the island contains forest, shrubs, and grass. The dune area is covered by the forest which consists of pinus, betula, and shrubs. The saltmarsh area is covered by herbs, sedges, rushes, and grasses (Schmidt and Skidmore, 2003). The marsh comprises 15 dominant species such as *Spartina, Artmesia maritime, Festuca rubra.* The variation of the saltmarsh's vegetation is caused by different factors such as, tidal regime, or climate that are directly and indirectly influenced by the saltmarsh's vegetation distribution (Schmidt et al., 2004). Figure **2.1** presents the vegetation types within Schiermonnikoog island.
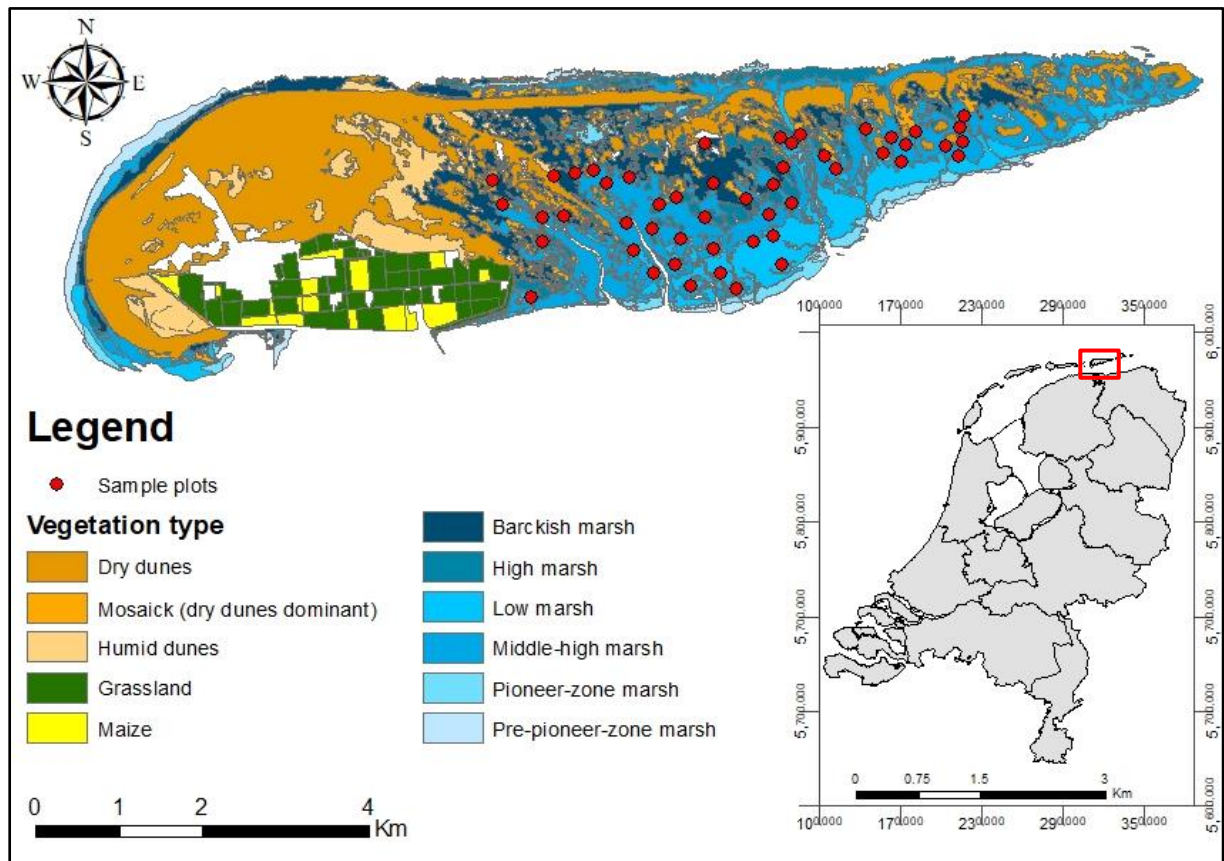

Figure 2.1. The map of the study area in Schiermonnikoog island, vegetation types, and visited sample plots

2.2.   Data

2.2.1.   Field data

A field campaign for collecting field data was conducted between 26th September and 5th October 2017. The test site stratified to 6 strata according to the existing vegetation types in the saltmarsh area of Schiermonnikoog island, which include Barckish_Marsh, Pre_pioneer_zone marsh, Pioneer_zone_marsh, Low_ marsh, Middle_high_marsh, High_marsh. Before visiting the test site, 100 plots randomly have been generated based on the vegetation cover map. To generate random plots, in ArcGIS 10.5.1, create random point tool from Arc Toolbox has been used. Nevertheless, because of limited time, budget, and inaccessibility, in 50 plots measurements were conducted.

In each plot of 20 by 20 meters, the coordinate of the centre were recorded using a GPS (Garmin eTrex 30X, ±2 m accuracy). To collect the representative samples of the plot, 5 subplots have been visited to collect leaf samples. To identify subplots, the strategy was to select the first subplot on the centre, the second in the north, the third in the south, the fourth one in the east, and the last one in the west directions.

Among the 50 plots, 24 plots were in the Middle_high_marsh area, 9 plots were in Barckish_Marsh area, 9 plots in the High_marsh area, and 8 plots in the Low_marsh area. Unfortunately, due to the weather and the site's condition, no data for Pre_pionner_zone marsh and Pioneer_zone_marsh could be collected.

In each sample plot, canopy coverage (%) by visual observation, and canopy height (cm) were measured. In addition, in each sample plot, for dominant species, leaf areas and their fresh weight were measured by digital balance. To measure the area of the leaves, the collected leaf samples were spread on a white surface, and beside them, a ruler was placed, then a picture in nadir direction has been taken. Consequently, the captured images were imported to ImageJ software to measure leaf sample areas.

After measuring leaf areas, the collected samples have been kept in a fridge in plastic bags. In departure time, to avoid of rotting samples, the water drops on their surface have been cleaned, and then the cleaned samples were placed in paper sample bags to transport to the laboratory. In the laboratory, the samples have been dried for 72 hours in the oven with 60°C, and after drying the samples, their dry mass has been measured through digital balance (Cornelissen et al., 2003). Therefore, by measuring these plant parameters, for further analysis, we were able to calculate the SLA values for each plot as $\frac{Leaf\ area\ (cm2)}{Leaf\ dry\ mass\ (g)}$ (Vile et al., 2005).

2.2.2.   Satellite data

The Sentinel-2 mission includes two identical satellite, Sentinel-2A and Sentinel-2B (Drusch et al., 2012). Sentinel-2A launched on 23rd June 2015 (Fernández-manso et al., 2016) and Sentinel-2B launched on 7th March 2017 (Monitoring, 2017). The Sentinel-2 mission main aims are to provide high-resolution multispectral imageries in a global scale with a high revisit repetition, and to provide data to obtain further products, for instance, estimation of biochemical and biophysical variables (Drusch et al., 2012). Sentinel-2 platforms include MultiSpectral Instruments (MSI) with 13 spectral bands, Sentinel-2 satellites cover spectrum range from visible and the near infrared to the shortwave infrared (van der Werff and van der Meer, 2016). In Table 2.1, some Sentinel-2 characterization of its MultiSpectral Instrument (MSI) is summarized.

In this study, nine high-resolution multispectral images of the Sentinel-2B satellite has been acquired which covers the whole area of Schiermonnikoog island, and it is captured on 15th September 2017. The images have been downloaded from the Copernicus website (https://scihub.copernicus.eu/). Then, the nine images were stacked to one image by using layer staking function in ENVI software. As it is mentioned in Section 2.2.1, the field campaign was conducted on 26th September 2017 till 5th October 2017; however, due to cloud coverage the most suitable (cloud-free) image belonged to 15th September 2017.

Table 2.1. Sentinel-2 spectral bands and their characteristics
(https://www.itc.nl/Pub/sensordb/getsat.aspx?name=Sentinel-2B)

Band	Spectral resolution (nm)	Bandwidth (nm)	Spatial resolution (m)
B1 (VIS)	443	20	60
B2 (VIS)	490	65	10
B3 (VIS)	560	35	10
B4 (VIS)	665	30	10
B5 (VIS)	705	15	20
B6 (VIS)	740	15	20
B7 (VIS)	775	20	20
B8 (NIR)	842	115	10
B8A (NIR)	865	20	20
B9 (NIR)	940	20	60
B10 (SWIR)	1375	20	60
B11 (SWIR)	1610	90	20
B12 (SWIR)	2190	180	20

3. METHODS

In this Chapter the processing steps on the downloaded Sentinel-2 image have been described and the settings for each statistical approach elaborated. At the end of this chapter, the calibration and validation set that have been used to evaluate statistical approaches have been explained.

3.1. The overall workflow of the methodology

In the following flowchart, the applied steps to achieve the research objectives of the present study have been shown (Figure 3.1).
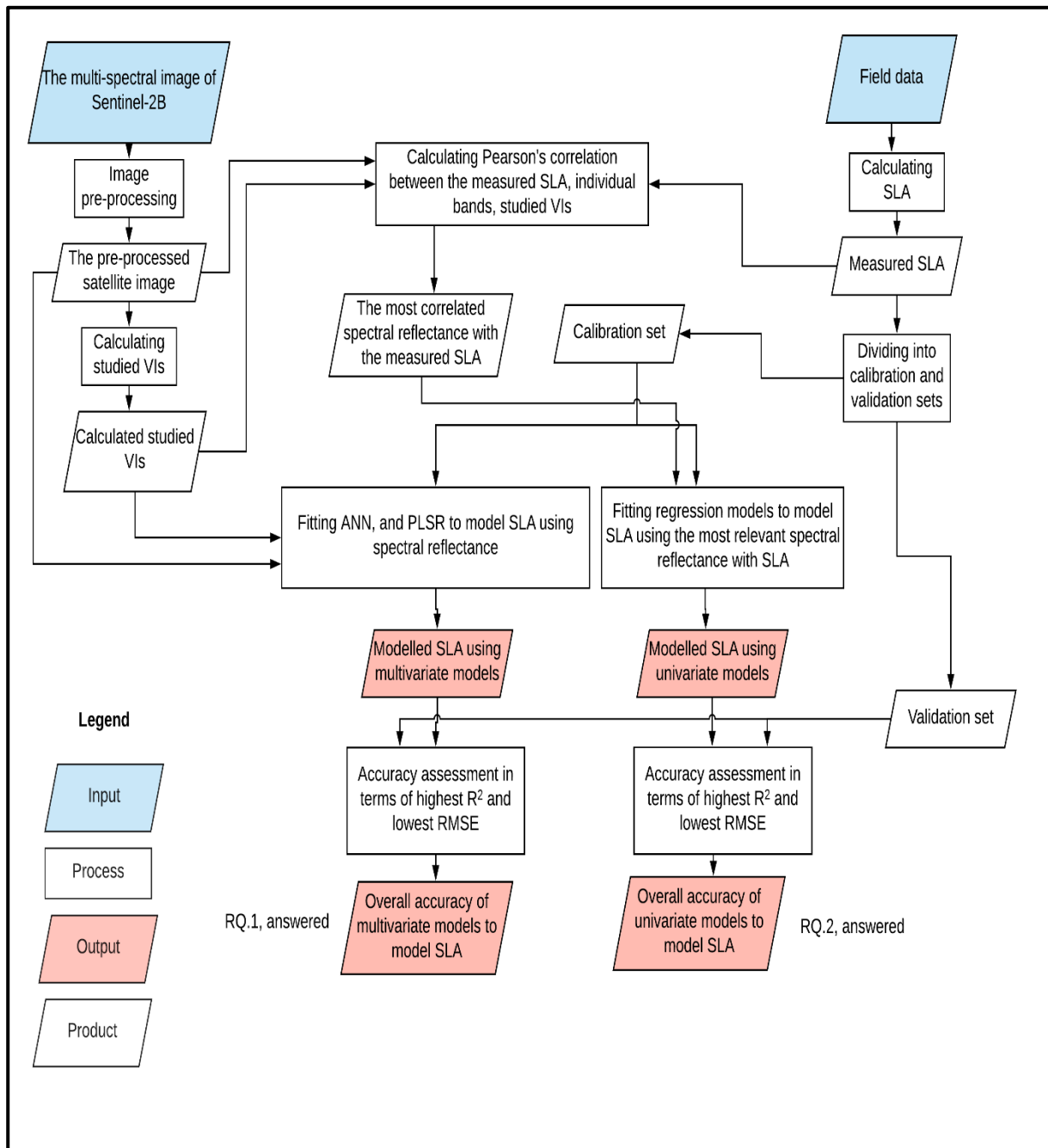
Figure 3.1. The general workflow of this study.

3.2.   Image pre-processing

The downloaded Sentinel-2B image have been pre-processed to calculate reflectance values of objects in the ground; for this purpose, the downloaded image should be atmospherically and radiometrically corrected. These processes are not only for obtaining reflectance values but also to eliminate the effect of cloud and atmospheric components that influence on the features' spectra (Bowker et al., 1985). The Sentinel-2 imageries are radiometrically corrected; therefore, only the atmospheric correction was needed in this study.

The acquired Sentinel-2B image has been atmospherically corrected by using Sen2cor 2.4.0 stand-alone software that developed to implement atmospheric, terrain, and cirrus correction of Top-Of-Atmosphere Level 1C input data (The European Space Agency (ESA), 2017). After that, the outputs of the process were three files of images which consist of spectral reflectance of Sentinel-2 bands with 10, 20, 60 meters resolutions. For this study, only bands with 20 meters resolution have been used. In several studies, it has been discussed that Red-edge and Near Infrared (NIR) regions provide appropriate information to estimate plant biophysical parameters (Asner, 1998; Darvishzadeh, 2008b; Filella and Penuelas, 1994; Foley et al., 1998; Horler et al., 1983; Lu et al., 2018). Therefore, Sentinel-2 images with 20 meters resolution which generally lay on Red-edge and NIR regions have been selected.

Subsequently, the pre-processed image has been converted from .jp2 format to .tiff format and their coordinate systems attached to .tiff files through ArcGIS 10.5.1. After that, the shapefile of the Schiermonnikoog boundary have been used to extract the same extent of the boundary of the raster file. Regarding the main objective which is modelling SLA in saltmarsh/ wetland ecosystem, the land-cover shapefile has been used to extract saltmarsh areas from other land-cover types (e.g. agricultural areas, dry dunes, humid dunes, mosaic (dry dunes dominant)).

3.3.   Statistical approaches to estimate SLA

3.3.1.   Vegetation Indices (VIs)

Vegetation Indices (VIs) have been implemented for different kind of applications (Ball et al., 2015b; Baret and Guyot, 1991; Darvishzadeh et al., 2009; Vrieling et al., 2017). In this study, several VIs have been calculated based on spectral bands of the downloaded Sentinel-2B image. The best VIs that accurately modelled Specific Leaf Area (SLA), and Leaf Dry Matter Content (LDMC) have been chosen according to previous studies (Ali et al., 2017a; Dorigo et al., 2009; Lymburner et al., 2000). The reason of choosing the VIs that accurately model LDMC is due to the strong correlation between SLA and LDMC in previous studies (Lobell et al., 2001; Nagler et al., 2003; Vile et al., 2005; Peter J Wilson et al., 1999).

However, some of the studied VIs have been conducted on hyperspectral imageries (Ali et al., 2016d; Dorigo et al., 2009). Therefore, in this study, those wavelengths of the spectrum were adjusted to Sentinel-2's wavelength (e.g. NMDI, CAI, SWIRVI). The pre-processed Sentinel-2 image has been utilized to compute VIs. After that, the correlation between measured SLA in the field and generated VIs have been evaluated. In this analysis, the Pearson method used to calculate the correlation coefficient (R). In this study, 9 spectral bands of Sentinel-2 which located in the visible and Near-infrared (NIR) regions as well as 11 VIs were utilized to estimate SLA. The selected vegetation indices are shown in Table 3.1.

The relation between spectral bands of Sentinel-2, and selected VIs with SLA have been examined and two statistical methods (univariate and multivariate) have been applied to estimate SLA in this study.

Based on the regression analysis in previous studies, the relationship between RS data (VIs and spectral bands) and measured SLA have been mostly modelled by linear and exponential regression methods (Ali et al., 2017b; Asner et al., 2011; Lymburner et al., 2000).

In this study, linear, quadratic, logarithmic, and exponential regression methods performed to estimate SLA via studied VIs. A linear regression model makes linear relationship between the dependent variable and the independent variable. While, a quadratic regression model makes 2nd degree polynomial (non-linear) relationship between the independent variable and the dependent variable. Logarithmic and exponential regression models make power predictive relationship between the independent variable and the dependent variable. Although VIs have been using to estimate SLA, multivariate models to our knowledge have not been utilized to estimate SLA. In this study, two most common types of multivariate models of RS applications (Corbane et al., 2013; Sunar Erbek et al., 2004; Yang et al., 2018; Yi et al., 2014) were assessed to model SLA.

3.3.2. Artificial Neural Network (ANN)

Among the different types of the neural networks, one of the most commonly used neural network is the multi-layer perceptron in RS applications (Atkinson and Tatnall, 1997). As indicated in Section 0, an ANN architecture usually includes of three layers (Inputs, hidden layers, output) (Hornik et al., 1989), the structure of an ANN is shown in Figure 3.2. The inputs in this study, included of individual spectral bands and studied VIs which obtained from the Sentinel-2 image, hidden layers that help the network to learn difficult tasks by continuously retrieving more meaningful pattern from inputs, and finally the output which is produced as response of the network (Haykin, 1999); moreover, to train the networks two different algorithm have been used (Levenberg-Marquardt, and Scaled Conjugate Gradient).

One of the problems in Multi-layer perceptron can be "Overfitting". "Overfitting" means the ANN model, based on training set obtained small error; while, applying the same model on test set, acquired a large error (Piotrowski and Napiorkowski, 2013). Therefore, to overcome the overfitting problem different techniques can be applied (e.g. model selection, early stopping, weight decay) which early stopping have been applied in this study (Lawrence et al., 1997). In early stopping technique, the training process will be stopped as soon as performance on test set starts to have higher error (Nowlan and Hinton, 1992). The calibrating and validating of ANN models have been repeated for 1000 times; and then, the average of repetitions has been taken. These iterations have been applied to reduce the effect of random initial optimization routine (Mirzaie et al., 2014).

In this study two sets of inputs as follow have been used to make neural networks: 1) The all individual spectral bands of the Sentinel-2 image. 2) The all studied VIs that selected to estimate SLA in this study. In the beginning, all values of inputs have been normalized, then they entered into models for further process.

Neural networks often have one or more hidden layers, and tan-sigmoid used as the transfer function for hidden layers; moreover, for the output layer, linear transfer function which is most used transfer function for function fitting (or non-linear regression) problems (Demuth et al., 2017). The linear transfer function helps networks to learn the non-linear relationships between input and output variables ("Multilayer Neural Network Architecture - MATLAB," 2018). Figure 3.2 shows a basic schema of an artificial neural network.
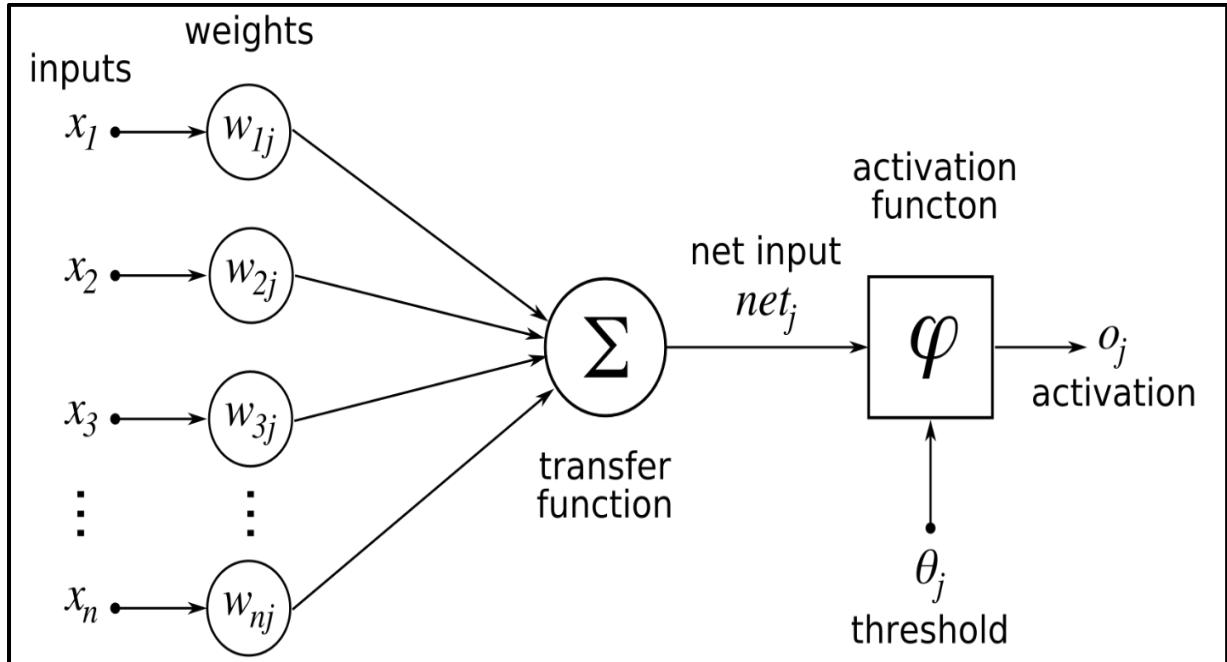
Figure 3.2. The schema of a basic artificial neural network
(http://andrewjamesturner.co.uk/ArtificialNeuralNetworks.php)

3.3.3. Partial Least Squares Regression (PLSR)

PLSR model is one of the popular multivariate models that converts the inputs (spectral information) to components (Helland, 1988). The main reason of the popularity of PLSR model is that this method can address and reduce the multicollinearity problem among independent variables (Abdi, 2003). The basics about PLSR fundamentals can be found in Williams and Norris, (1987). PLSR model have been used for RS studies (Carrascal et al., 2009; Cho et al., 2007; Kooistra et al., 2004); moreover, PLSR have been used to estimate biochemical and biophysical parameters through RS data (Asner and Martin, 2008; Darvishzadeh, 2008b; Li et al., 2014; Mirzaie et al., 2014; Ullah et al., 2014). In this study, PLSR model have been developed for two different sets of explanatory variables: 1) The all individual spectral bands of Sentinel-2 image, and 2) The chosen VIs in this study to estimate SLA; and then, a different number of components were validated to find the optimal number of components.

The calculated RMSE for each PLSR models have been evaluated to find the optimal number of components, the criterion to select the optimal number for components is that by adding an extra component to a PLSR model, the RMSE decreases by >2% (Geladi and Kowalski, 1986); in addition, visual inspection of the validation plot between the measured SLA and the predicted SLA has been used. For this aim, SelectNcomp function in R software used to find the optimal number of components for a PLSR model. Then, to evaluate PLSR models the same calibration and validation sets have been used.

Table 3.1. Table of studied vegetation indices in this study

Vegetation indices	Description	Formula	Reference
NMDI	A Normalized Multi-Band Drought Index	$\dfrac{NIR - (SWIR_{1610nm} - SWIR_{2190nm})}{NIR + (SWIR_{1610nm} - SWIR_{2190nm})}$	(Wang and Qu, 2007)
SLAVI	Specific Leaf Area Vegetation Index	$\dfrac{NIR}{(Red + SWIR_{1610nm})}$	(Lymburner et al., 2000)
VARI	Visible Atmospherically Resistant Index	$\dfrac{(Green - Red)}{(Green + Red - Blue)}$	(Gitelson et al., 2002)
SAVI	Soil-Adjusted Vegetation Index	$[\dfrac{(NIR - Red)}{(NIR + Red + L)}](1 + L *)$	(Huete, 1988)
RVI	Ratio Vegetation Index	$\dfrac{NIR}{Red}$	(Jordan and Society, 1969)
NDVI	Normalized Difference Vegetation Index	$\dfrac{(NIR - Red)}{(NIR + Red)}$	(Rouse, J. W. et al., 1974)
GNDVI	Green Normalized Difference Vegetation Index	$\dfrac{(NIR - Green)}{(NIR + Green)}$	(Gitelson et al., 1996)
SARVI2	Soil and Atmosphere Resistant Vegetation Index	$\dfrac{2.5 * (NIR - Red)}{(1 + NIR + (6 * Red) - (7.5 * Blue))}$	(Huete et al., 1997)
NDMI	Normalized Difference Moisture Index	$\dfrac{(NIR - SWIR_{1610nm})}{(NIR + SWIR_{1610nm})}$	(Ali et al., 2017a)
CAI	Cellulose Absorption Index	$(0.5*(SWIR_{1610nm} + SWIR_{2190nm})) - SWIR_{1610nm}$	(Nagler et al., 2003)
SWIRVI	Shortwave Infrared Green Vegetation Index	$37.27*(SWIR_{2190nm} - SWIR_{1610nm}) + 26.27 * ((SWIR_{2190nm} - SWIR_{1610nm}) + 0.57$	(Lobell et al., 2001)

∗ Which L can vary between 0-1 and its value depends on vegetation density

3.4. Calibration and validation

After performing different statistical methods (univariate and multivariate) to model SLA, evaluating the model performances were needed. For this aim, the entire collected dataset were splited into two sets which were calibration and validation sets. Therefore, 60% of the dataset randomly assigned to calibration set (30 plots) and 40% of the dataset randomly allocated to validation set (20 plots).

Subsequently, 60% of the dataset used to calibrate the all performed models; after that, the fitted models have been evaluated through 40% of the dataset. For each model, R^2 and RMSE have been. The R^2 and RMSE for different models have been investigated, and their results were reported in Section 4.4.

The following formulas have been used to calculate R^2 and RMSE:

1) $R^2 = 1 - \dfrac{\sum(y_i - y_i')^2}{\sum(y_i - \bar{y})^2}$

2) $RMSE = \left(\sqrt{\dfrac{\sum(y_i - y_i')^2}{n}} \middle/ \bar{y} \right)$

Which in these formulas, y_i and y_i' are the actual and predicted values of SLA for sample with number i; in addition, n is the number of samples in the measured dataset. Moreover, $\bar{y}$ is the average of measured dataset.

4. RESULTS

In this chapter, the results of the performed analysis are presented. These include the statistics of the measured plant parameters and a summary of their respective correlations. Further, the performance of different statistical models (VIs, ANN, PLSR) to model SLA have been presented and examined.

4.1. The descriptive statistics of measured plant parameters

Summary statistics of the measured plant parameters (Specific Leaf Area (SLA), Leaf Area (LA), and Leaf Dry Matter Content (LDMC), canopy height, canopy coverage) in Schiermonnikoog island are presented in Table 4.1. As it is shown in Table 4.1, the range of SLA values varied between 69.78 (cm²/g) to 340.56 (cm²/g) with a mean of 131.82 (cm²/g). The maximum and the minimum LA value recorded in the field were 172.11 (cm²), and 60.71 (cm²) respectively. Further, the LDMC value ranged between 0.34 (g) and 1.28 (g). As shown in Table 4.1, the maximum recorded canopy height was 100 (cm). According to the results demonstrated in Table 4.1, canopy height (CV=0.37) had the highest variability compared to the other measured plant parameters.

Table 4.1. The descriptive statistics of measured variables in Schiermonnikoog island (n=50)

Parameters	Canopy height (cm)	Canopy coverage (%)	SLA (cm²/g)	Leaf Area (LA) (cm²)	Leaf Dry Matter Content (LDMC) (g)
Mean	52.24	67.8	131.82	116.18	0.94
Maximum	100	90	340.56	172.11	1.28
Minimum	2.00	30.00	69.78	60.71	0.34
Standard Deviation	19.44	13.29	42.16	23.23	0.20
Range	98	60	270.78	111.4	0.94
Coefficient of Variation (CV)	0.37	0.20	0.32	0.20	0.22

4.2. The correlation between measured plant parameters

The Pearson's correlation coefficients between the measured plant parameters (SLA, LA, LDMC, canopy coverage, canopy height) have been presented in Table 4.2. As indicated in Table 4.2, there is a weak correlation between the measured SLA and the measured LA ($r = 0.17$). In contrast, there is a strong negative correlation between the measured SLA and the measured LDMC ($r = -0.73$). The correlation between the measured LA and LDMC values was $r = 0.37$. The correlations of canopy height with LDMC and LA were found to be 0.45 and 0.65 respectively. Further, the correlations of canopy coverage with LDMC and LA were found to be 0.21 and 0.13 respectively. Moreover, the correlation between SLA and

canopy coverage was found to be (r = 0.66); lastly, SLA had a weak correlation with canopy height (r = 0.19).

Table 4.2. The correlation between measured variables in Schiermonnikoog island (n=50)

Measured plant parameters	SLA (cm²/g)	LA (cm²)	LDMC (g)	Canopy height (cm)	Canopy coverage (%)
SLA	1				
LA	0.17	1			
LDMC	-0.73*	0.37	1		
Canopy height	0.19	0.65*	0.45	1	
Canopy coverage	0.66*	0.13	0.21	0.11	1

* P ≤ 0.05

4.3.   The correlation between the measured SLA, spectral bands, and studied VIs

The correlations between Sentinel-2 reflectance data (Individual bands and studied Vegetation Indices (VIs)) and the measured SLA were investigated using Pearson's correlation coefficient (r). The reason for performing this analysis was to identify the most relevant spectral band/ index for estimating SLA.

As it is mentioned in Section 3.3.1, the VIs were chosen based on their performances in SLA and LDMC estimation in previous studies (e.g. Ali et al (2017); Lobell et al., (2001); Lymburner et al., (2000); Wang and Qu, (2007)). The calculated Pearson's correlations coefficient (r) between the measured SLA and the Sentinel-2 spectral bands are presented in Figure 4.1. As it is shown in Figure 4.1, the strongest correlation was found between the measured SLA and bands 8A and 6 of the Sentinel-2 image (r = 0.35, r = 0.35 respectively). The obtained correlations between the measured SLA and the spectral bands of Sentinel-2 shows that SLA is sensitive to Near InfraRed (NIR) and Red-edge region of the spectrum. In addition, as can be seen in Figure 4.2, Among the studied VIs strongest correlation was found between the Ratio Vegetation Index and the measured SLA (r = 0.45).
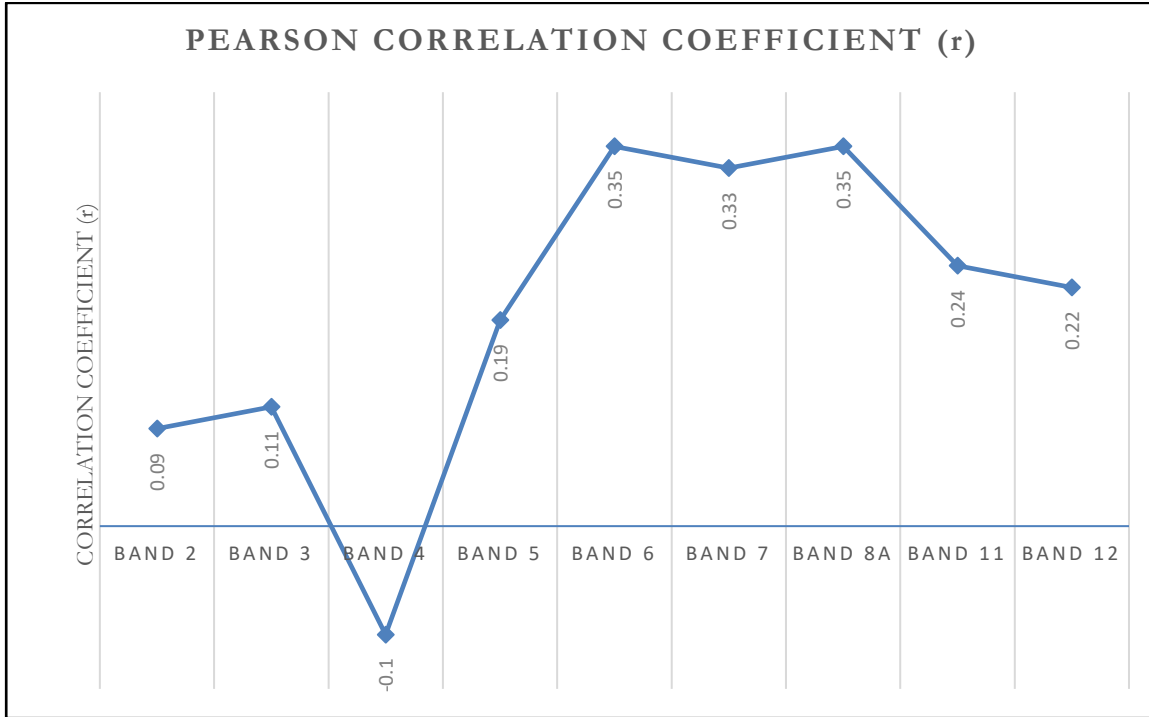
Figure 4.1. The Pearson's correlation coefficient (r) between measured SLA and individual bands of Sentinel-2B image of 15th September 2017 in Schiermonnikoog island (n=50)
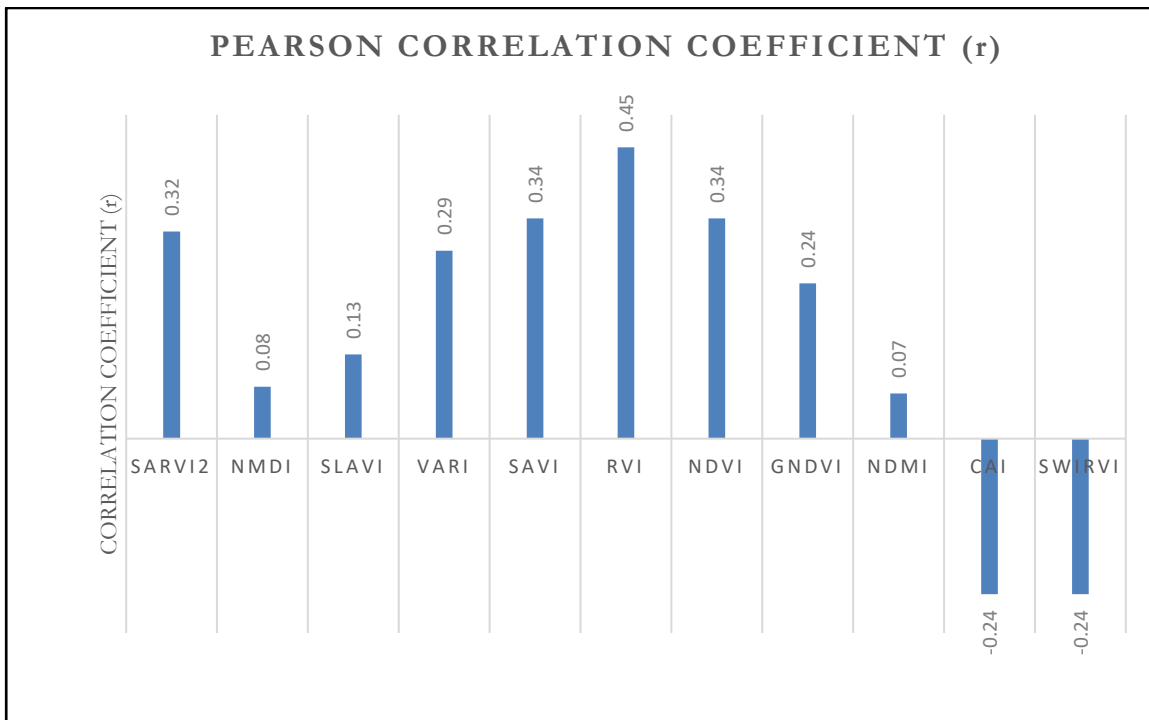
Figure 4.2. The Pearson's correlation coefficient (r) between measured SLA and studied VIs of Sentinel-2B image of 15th September 2017 in Schiermonnikoog island (n=50)

4.4.   The results of statistical approaches to estimate SLA

4.4.1.   The result of VIs

Based on the results obtained from the calculated Pearson's correlation coefficient (r) between the measured SLA and the spectral reflectance of Sentinel-2; RVI (with the strongest correlation with the measured SLA) was used to estimate SLA by using linear, quadratic, logarithmic, and exponential regression models. As mentioned in Section 3.4, 60% of the field dataset (30 samples) was used to calibrate the models, and 40% of the field dataset (20 samples) was used as an independent dataset to validate the same. Further, it bears emphasis that the same calibration and validation dataset were used for all regression models.

The results of SLA estimation using RVI have been shown in Table 4.3. As can be observed in Table 4.3, using the validation dataset; the simple linear regression acquired the highest R^2 and the lowest RMSE between the measured and predicted SLA (0.46 and 0.64 respectively), while the calibration dataset also returned the high R^2 and the low RMSE of 0.61 and 0.51 respectively. The relationship between the measured and the predicted SLA using RVI through simple linear regression regard to validation set was shown in Figure 4.3. In Figure 4.3, the solid line presents the one to one relationship between the predicted SLA and the measured SLA.

Table 4.3. The acquired R^2 and RMSE between measured and predicted SLA using different types of regression models for calibration and validation set

Bands/VIs	Type of the regression model	Calibration (n=30)		Validation (n=20)	
		R^2	RMSE	R^2	RMSE
RVI	**Linear**	**0.61**	**0.51**	**0.46**	**0.64**
	Quadratic	0.64	0.58	0.40	0.65
	Exponential	0.71	0.56	0.38	0.67
	Logarithmic	0.57	0.55	0.42	0.66
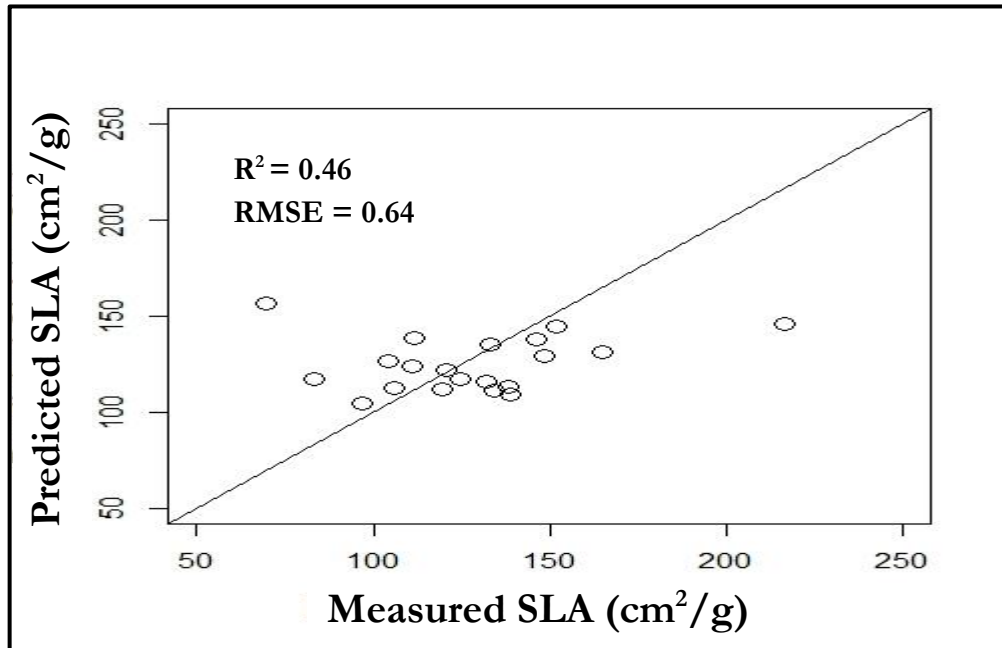
Figure 4.3.The relationship between measured and predicted SLA using RVI index and linear regression model. The SLA values are based on the validation dataset

4.4.2. The result of ANN

As mentioned in Section 0, in this study the following two methods, Levenberg-Marquardt (LM) and Scaled Conjugate Gradient (SCG) were utilized to train the neural networks (Demuth et al., 2017). As inputs to neural networks, two sets of RS data were used. First set was all individual bands of Sentinel-2, and the second set was all studied VIs. Several studies have mentioned that using a higher number of hidden layers increases the ability of ANN models to solve complex problems (Atkinson and Tatnall, 1997; Skidmore et al., 1997); nonetheless, there is no unique rule to identify the optimal number of hidden layers (Fortuna et al., 2001). Therefore, a different number of hidden layers have been tested. The optimal number of hidden layers acquired by testing neural networks of varying depths have been shown in Table 4.4 (regarding their inputs and training methods).

As illustrated in Table 4.4, the highest accuracy to estimate SLA (in terms of high R^2 and low RMSE (0.55, 0.47 respectively) was obtained by the neural network which used all studied VIs as input and the Levenberg-Marquardt method for training the network parameters. In addition the optimal number of hidden layers was found to be 5. Further, as displayed in Table 4.4, the highest R^2 to estimate SLA ($R^2 = 0.66$, RMSE = 0.56) has been acquired by the neural network that used all individual bands of Sentinel-2 as input (regarding to calibration set).

In the experiments carried out to determine the optimal depth of the neural network, it was observed that upon increasing the number of hidden layers the R^2 increases but the associated RMSE increases as well. This observation indicates the possibility of the neural network over-fitting the training data (Bourquin et al., 1998); and therefore a careful selection of the network depth is essential to mitigate this problem. The relation between the measured and the predicted SLA using the most accurate ANN model found in the course of the analysis is shown in Figure 4.4. The solid line in Figure 4.4 indicates the one to one relationship between measured and predicted values of SLA.

Table 4.4. The acquired R^2 and RMSE between measured and predicted SLA using different types of training algorithms

Input	Optimal number of hidden layers	Output	Training algorithms	Calibration (n=30)		Validation (n=20)	
				R^2	RMSE	R^2	RMSE
All individual bands of Sentinel-2 (9 bands)	5	1	LM	0.62	0.55	0.49	0.50
	6	1	SCG	0.66	0.56	0.48	0.49
All studied VIs	**5**	**1**	**LM**	**0.56**	**0.57**	**0.55**	**0.47**
	4	1	SCG	0.56	0.54	0.43	0.60
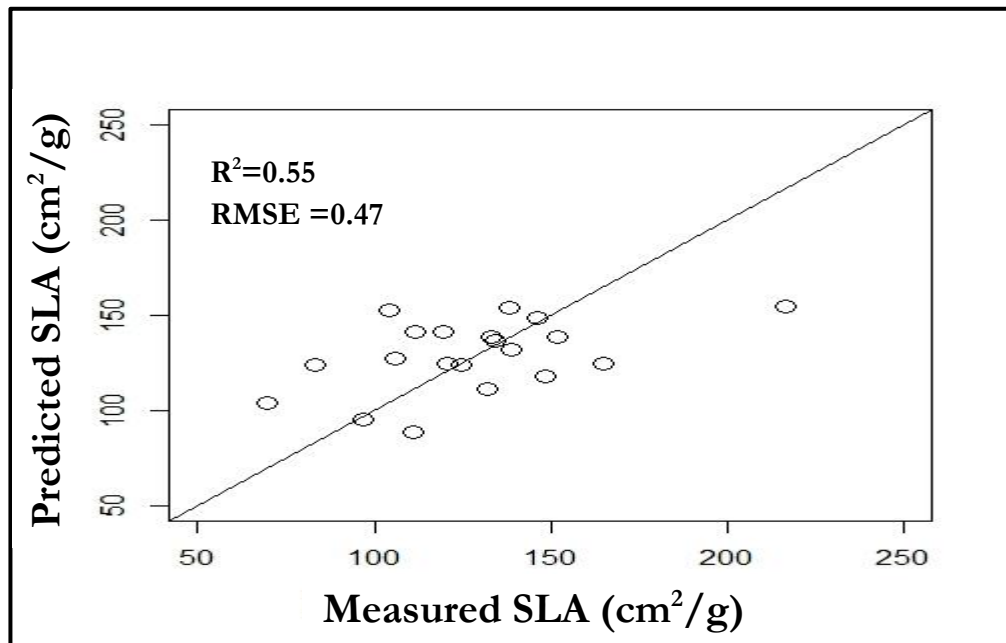
Figure 4.4.The relationship between measured and predicted values of SLA by the ANN model (training method= LM, optimal hidden layers=5 using all studied VI as inputs).

4.4.3. The result of PLSR

In the present study, Partial Least Square Regression (PLSR) method has been evaluated to estimate SLA. One of the differences between PLSR models was inputs that were used to build the PLSR models. The same calibration and validation dataset were used to model SLA by PLSR models. The first PLSR model included all individual bands of Sentinel-2 image as inputs. As it is shown in Table 4.5, the optimal number of components for this model was 4. The acquired R^2 and RMSE between the measured and the predicted SLA using the PLSR model were 0.44 and 0.48 respectively (based on the validation set).

In the second PLSR model, all studied VIs were used as inputs. We obtained R^2 and RMSE between the measured and the predicted SLA were 0.46 and 0.42 respectively. As reported by Geladi and Kowalski, (1986), the criterion to add an extra component is that the additional component decreases the RMSE based on the validation set by >2%. As it is shown in Figure 4.5, the optimal number of the components were identified through the visual inspection and the indicated criterion. Moreover, Figure 4.6 illustrates the predicted SLA values against the measured SLA values based on the PLSR model that utilized all VIs as inputs to estimate SLA by using 5 components (according to the validation set).

Table 4.5. PLSR models in terms of R^2 and RMSE between measured and predicted SLA

Bands/VIs	Optimal Number of components	Calibration (n=30)		Validation (n=20)	
		R^2	RMSE	R^2	RMSE
All individual bands of Senitnel-2 (9 bands)	4	0.63	0.61	0.44	0.48
All studied VIs of Senitnel-2(11 VIs)	**5**	**0.70**	**0.60**	**0.46**	**0.42**
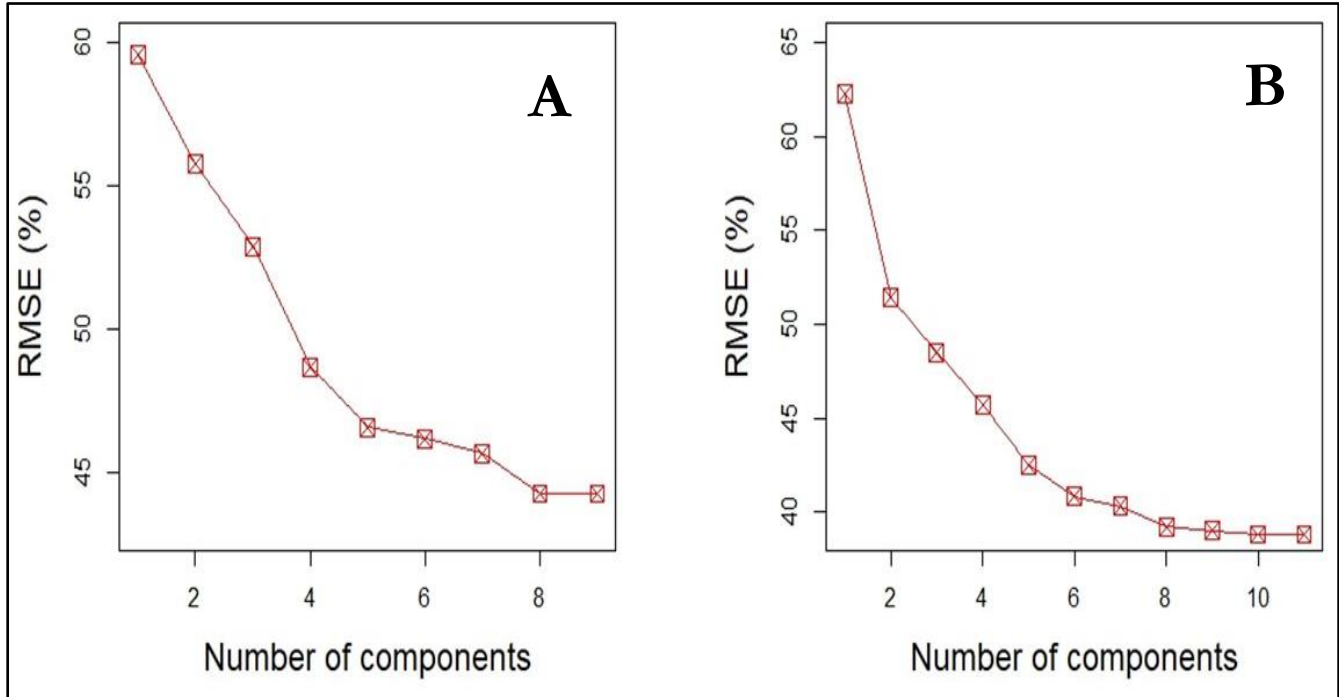
Figure 4.5.Percentage of RMSE against the number of components. (A) the PLSR model that used all individual bands as input (B) the PLSR model that used all studied VIs as input
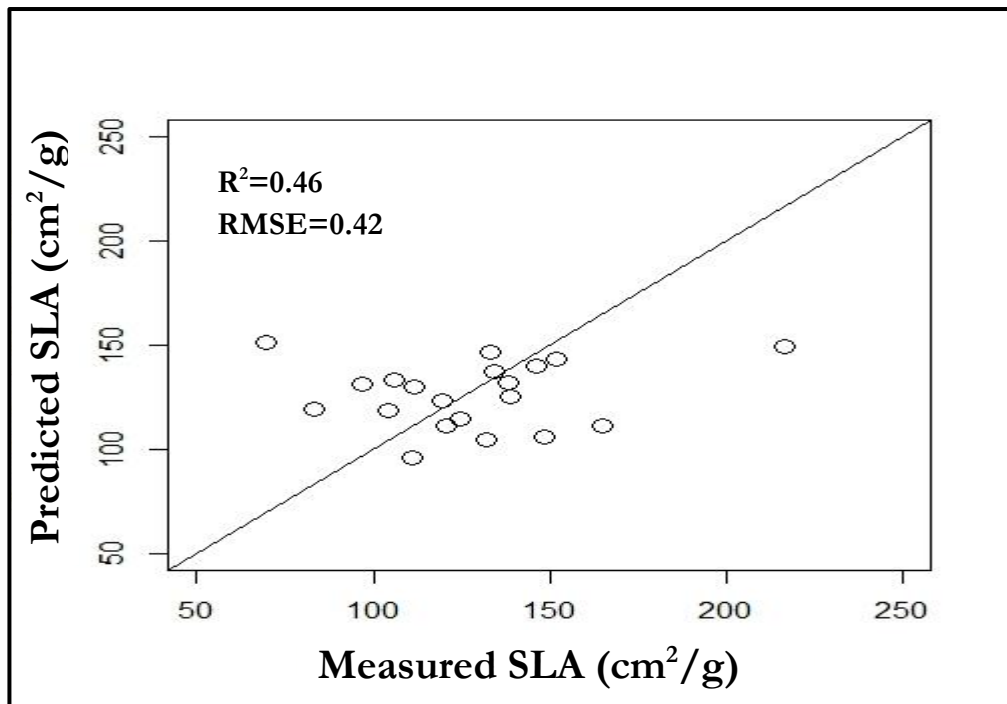
Figure 4.6. The predicted values of SLA by the PLSR model (Optimal number of components=5) and measured values of SLA using all studied VI.

5. DISCUSSION

In this chapter the performances of SLA estimation using Sentinel-2 data through different statistical models (VIs, ANN, PLSR) have been discussed. In addition, the limitations that led us to get our result have been described in this chapter. Moreover, the relevant studies have been reviewed, and their results have been compared to our results.

5.1.   The descriptive statistics and correlation of measured plant parameters

In this section, the result of descriptive statistics and the calculated Pearson's correlation coefficient between measured plan parameters have been discussed. Furthermore, the results of relevant literature have been described as well.

The measured SLA in this study ranged between 69.78 and 340.56 (cm²/g) that was in agreement with earlier studies which have investigated on similar ecosystems. For instance, McCoy-Sulentic et al., (2017) who studied woody and herbaceous species along the Colorado River in Arizona, reported that the measured SLA were ranged from 50 to 400 (cm²/g). In another study, Liu et al., (2017) investigated on SLA changes based on four different types of species in temperate grasslands in northern China; and reported that the measured SLA was ranged between 50 to 350 (cm²/g). Moreover, regarding results presented in Table 4.1, the Coefficients of Variation (CV) were calculated for SLA, LA, and LDMC in this study (0.32, 0.20, and 0.22 respectively). These findings show that the variation in collected SLA is higher than variation in collected LA and LDMC which means the SLA data are not closely distributed around the averaged SLA (mean of SLA values = 131.82 (cm²/g)) (Figure 5.1).

Figure 5.1. The distribution of SLA values in Schiremonnikoog island (n=50).

As it is shown in Section 4.2, in general, SLA had a strong correlation with LDMC; nevertheless, the correlation between SLA and LA was weak. One of the reasons of weak correlation between SLA and LA might be due to the errors that happened during the leaf area measurements through ImageJ software; errors mostly happened due to two conditions: 1) The shadows during capturing pictures resulted us in overestimating the leaf area measurements, 2) Overlying the leaf samples on top of each other led us to underestimate the 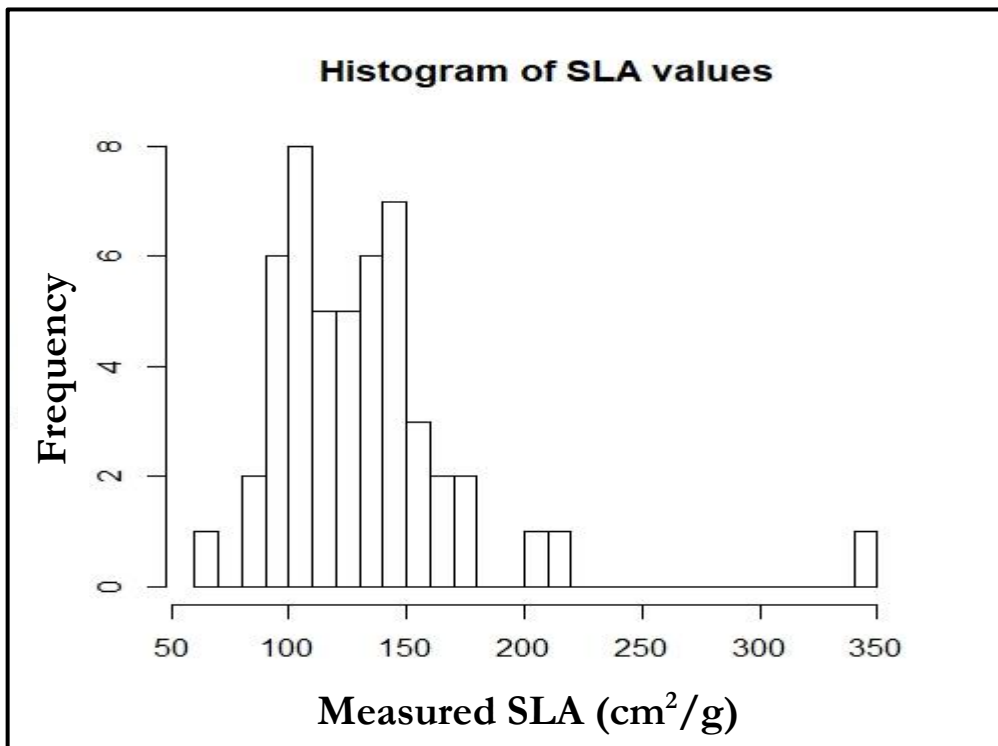leaf area measurements. Another reason for the weak correlation between SLA and LA in our study might be due to the exitance of different species. Ackerly et al., (2002) investigated on the relation between leaf size, SLA, and microhabitat of woody and herbaceous plants in Jasper Ridge Biological Preserve, San Mateo, California; they reported that the correlation between SLA and leaf size of woody and herbaceous plants is weak across several species. This result also confirms the findings of an earlier study by Vernescu and Ryser, (2009) who investigated the constraints on leaf structural traits in wetlands and reported that there was not a strong correlation between LA and SLA in wetland's plants.

The strong negative correlation between SLA and LDMC which was observed in this study is in agreement with previous findings by Wilson et al., (1999) who studied the leaf dry matter content and SLA as predictors for plant strategies based on different types of native British flora; according to their findings, there was a strong negative correlation between SLA and leaf dry matter content. Further Vernescu and Ryser, (2009) reported a strong positive correlation between leaf size and leaf dry matter content. In addition, the study by Vile et al., (2005) who investigated on the influence of SLA and LDMC to estimate leaf thickness in laminar leaves at three Mediterranean climate sites, indicated that there is a strong negative correlation between SLA and LDMC.

In conclusion of this section, SLA and LDMC had strong negative correlation; while, SLA and LA had a weak positive correlation. The main reason of weak correlation between SLA and LA is the heterogeneity of the ecosystem that influenced on the correlation between SLA and LA.

5.2. The correlation between spectral bands and studied VIs with the measured SLA

In this section, the Pearson's correlation coefficient between the reflectance of Sentinel-2 spectral bands, studied VIs and measured SLA are discussed.

Among the studied VIs in this study, RVI calculated from the reflectance of Sentinel-2 spectral bands were strongly correlated to SLA (r = 0.45). The result was in agreement with the previous study by Lymburner et al., (2000) who found that the RVI was one of the VIs which accurately estimates SLA. Furthermore, several studies (Ali et al., 2017b, 2017c; Lymburner et al., 2000) have shown the importance of Near Infra-Red (NIR) region of the spectrum to estimate SLA; in addition, as shown in Figure 4.1, NIR and Red-edge regions of spectrum are correlated to SLA stronger than other spectral regions.

We further, investigated whether species heterogeneity has affected the correlation between studied VIs and SLA and if stratification will improve the relation. For this aim, literature about vegetation coverage in Schiermonnikoog island have been reviewed (Schmidt et al., 2004; Vrieling et al., 2017). Stratification of vegetation classes has been considered based on the dominant species in each vegetation class. The dominant species in Highmarsh and Barckishmrash were **Festuca rubra, Elytriagia atherica**; while, in Middlemarsh and Lowmarsh were mostly covered by **Puccinellia maritima** (Figure 5.2, Figure 5.3, Figure 5.4). Therefore, vegetation classes were grouped into following two vegetation classes: 1) HMBM: Highmarsh and Barckishmarsh (n=17), 2) MMLM: Middlemarsh and Lowmarsh (n=33).

We observed that the heterogeneity of species in HMBM plots were higher than species in MMLM plots. In HMBM plots, 7 out of 17 plots were contained more than one species; while, in MMLM plots, only 5 out of 33 plots were contained more than one species. Regarding the results presented in Table 5.1, the correlation between SLA and LA in HMBM class is weak ($r = 0.13$). This finding confirmed by Ackerly et al., (2002)'s study which reported in plots with the higher heterogeneity of species the relation between SLA and LA is weak; nonetheless, the correlation between SLA and LA in MMLM class is stronger ($r = 0.41$). The reason for the stronger correlation between measured plant parameters in MMLM class compared to HMBM class might be the variation of species in plots as indicated earlier.

Table 5.1.The Pearson's correlation coefficient (r) between measured plant parameters according to type of vegetation cover in Schiermonnikoog

Parameters(HMBM)(n=17)	SLA (cm²/g)	LA (cm²)	LDMC (g)
SLA	1		
LA	0.13	1	
LDMC	-0.82*	0.36	1
Parameters(MMLM)(n=32)	SLA (cm²/g)	LA (cm²)	LDMC (g)
SLA	1		
LA	0.41	1	
LDMC	-0.50	0.55	1

* P ≤ 0.05

Figure 5.2. (A) High-marsh and (B) Barckish-marsh vegetation cover classes covered by **Elytriagia atherica** as the dominant species.

Figure 5.3. (C) High-marsh and (D) Barckish-marsh vegetation cover classes covered by **Festuca rubra** as the dominant species.

Figure 5.4. (E) Lowmarsh and (F) Middlemarsh vegetation cover classes covered by **Puccinellia maritima** as the dominant species.

Regarding to the obtained results showed in Figure 5.5, it has been reaveled that analysis based on vegetation cover classes would not help to improve the correlation between the measured SLA and the studied SLA. The reasons of acquired results (based on vegetation cover classes) might be the high percentage dried material and the influence of background material on derived spectral reflectance.
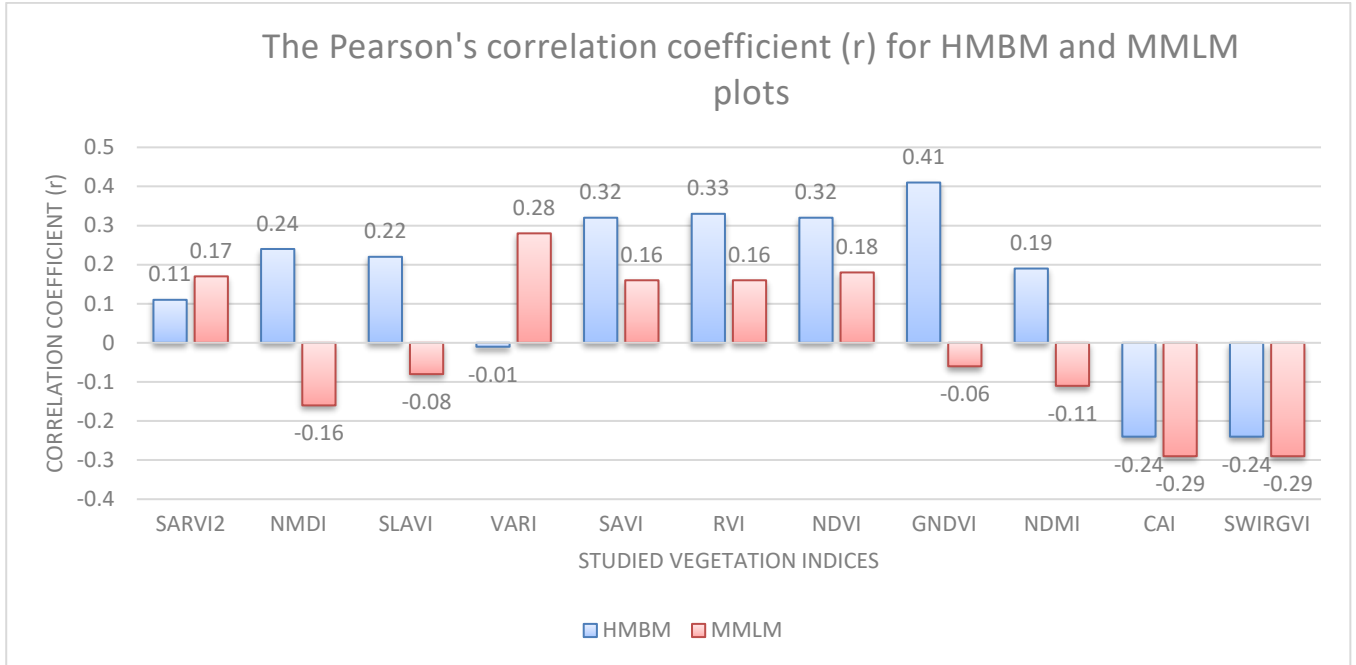
Figure 5.5.The Pearson's correlation coefficient (r) between measured SLA and studied VIs in HMBM (n=17) and MMLM (n=33) plots.

5.3. The result of statistical models (univariate and multivariate) to estimate SLA

In this section, the performance of different statistical models has been discussed. In addition, the results of this study explored to realize the relationships between measured SLA values and predicted SLA values through different models.

5.3.1. Vegetation Indices (VIs)

Among the studied models, the linear regression model using RVI as the independent variable obtained the highest R^2 and the lowest RMSE (0.46, 0.64 respectively) using the validation dataset. This finding is confirmed by previous studies that reported the linear regression using VIs will be the accurate model to estimate SLA. As Lymburner et al., (2000) reported that SLA could be estimated accurately through linear regression using RVI as the independent variable ($R^2 = 0.91$); moreover, Ali et al., (2017b) reported, Enhanced Vegetation Index (EVI) as the independent variable that linearly and accurately can estimate SLA among the all its studied VIs ($R^2 = 0.77$, RMSE (%) = 4.44). Nevertheless, regarding to the obtained results that were presented in Section 4.4.1, the SLA modelling through univariate models in this study is not as accurate as SLA modelling in previous studies.

One reason might be the wetland ecosystem which consists of variety of species. Another reason might be due to the existence of dried materials in most plots which sometimes were 60% of coverage in a plot. Moreover, 10 plots had low canopy coverage which caused the influence of background materials on spectral reflectance to be more pronounced. Although, VIs have been used to reduce the errors that caused by atmospheric and background materials (Hatfield et al., 2008), the effect of background materials had an impact on spectral reflectance and calculated VIs.

5.3.2. Artificial Neural Network (ANN)

Although, most studies that have been used ANN models benefited from hyperspectral data; in our study, the performance of studied VIs and the spectral bands of Sentinel-2 to estimates SLA were investigated. In the following paragraphs, the results of relevant literature have been described.

The highest R^2 and the lowest RMSE (0.55, 0.47 respectively) have been obtained by the AAN which consisted of 11 VIs as inputs, 5 as an optimal number of hidden layer, and Levenberg-Marquardt as training algorithm. The results confirm earlier results by Li et al., (2011) who studied different multivariate models to classify land-cover in a moist tropical region of Brazil using Landsat TM imagery. Li et al., (2011) used some vegetation indices and textural images that derived from Landsat TM images. They found that when six spectral bands of Landsat TM were used to build ANN model, the ANN model (overall accuracy = 52.1) obtained lower accuracy compared to the ANN model (overall accuracy = 70.7) which used a combination of VIs and two textural images.

Also, Yuan et al., (2017) investigated the retrieval of Leaf Area Index (LAI) for soybean using a number of models including ANN and PLSR models. They reported that the highest accuracy were obtained by ANN based on stratified sampling set over single growth phase.

5.3.3. Partial Least Square Regression (PLSR)

The PLSR model with 5 components using VIs as inputs, acquired the highest R^2 and the lowest RMSE in both calibration and validation sets (Calibration: $R^2 = 0.70$, RMSE = 0.60 and Validation: $R^2 = 0.46$, RMSE = 0.42). This result confirms the findings of the earlier studies which have investigated the estimation of vegetation parameters through PLSR model (e.g. Cho et al., 2007, Darvishzadeh et al., (2011), Hansen and Schjoerring, 2003, Siegmann and Jarmer, 2015, Wolter et al., 2009,).

For example, Cho et al., (2007) studied the estimation of green grass/herb biomass through univariate and multivariate models and reported that among the applied regression models, PLSR obtained the lowest standard error prediction (SEP=149 g m-2). In another study, Wolter et al., (2009) investigated the estimation of forest structural parameters using PLSR in conifer and hardwood covers and found that PLSR models in both conifer and hardwood areas performed accurately to estimate forest structural parameters.

5.3.4. PLSR *vs* ANN

In this section, the comparison between performed ANN and PLSR models have been explained. Moreover, the results of this study have been compared to findings from relevant literature.

Li et al., (2016) studied on the grassland LAI prediction in the meadow steppes of northern china through hybrid geostatistical models (regression kriging and random forests residuals kriging) and regression models (random forest, partial least square regression, artificial neural network). They reported the PLSR as the worst performed model to predict grassland LAI compared to other studied regression models.

Yuan et al., (2017) also showed to retrieve soybean leaf area index from UAV hyperspectral data using different regression models (random forest, support vector machine, artificial neural network, and partial least square regression) the PLSR model inaccurately retrieve soybean LAI comparted to the other studied models. Chen and Jing, (2017) studied winter wheat forecasting using Landsat-8 OLI images through two multivariate regression models (ANN and PLSR) and concluded that the PLSR model ($R^2=0.39$, RMSE (%)= 12.84) did not perform accurately compared to ANN ($R^2=0.61$, RMSE (%)= 10.38) model.

However, in other studies, PLSR models have shown to perform more accurate compared to other multivariate regression models. For example, Farifteh et al., (2007) studied the prediction of soil salinity using soil reflectance through PLSR and ANN and observed that PLSR models had similar performance with ANN. Also, Mirzaie et al., (2014) investigated the estimation of Vegetation Water Content (VWC) through univariate and multivariate models and found that PLSR model is capable of estimating VWC accurately than other regression models including ANN.

In conclusion of Section 5.3, among the studied VIs, RVI performed accurate modelling to model SLA; moreover, the accurate regression model using RVI of Sentinel-2 was simple linear regression model. In addition, among the studied multivariate models, the highest accurate model was the ANN model that included 11 VIs as input, 5 as an optimal number of hidden layer, and Levenberg-Marquardt as training algorithm.

6.   CONCLUSION AND RECOMMENDATIONS

6.1.   Conclusion

From the current study, the following conclusions were derived:

- In this study, the correlation between SLA and LA was weak due to species variation in each plot. However, a higher correlation has been identified between SLA and LDMC.

- To estimate SLA, Sentinel-2 data provide accurate information, although for improving the acquired results to estimate SLA in this study, the number of samples shall be increased.

- Both bands 8A and 6 were strongly correlated to the measured SLA compared to other selected bands; moreover, among the studied VIs, RVI had a strong correlation with the measured SLA which led us to use RVI to model SLA through different regression models.

- Between different regression models using RVI, simple linear regression has performed accurately than other regression models to estimate SLA.

- Among the studied multivariate models, ANN using all studied VIs acquired an accurate estimation of SLA in saltmarsh/ wetland ecosystem.

6.2.   Answers to research questions

Q1. Among the studied vegetation indices, which index will more accurately (Highest R^2 and lowest RMSE) model SLA in Schiermonnikoog using Sentinel-2 data?

Answers: In this study, using RVI as the independent variable, obtained the strongest correlation between the measured SLA and the predicted SLA through the linear model in schiermonnikoog island (R^2 = 0.46, RMSE = 0.64).

Q2. Among the studied multivariate models (ANN, PLSR), which model will accurately model SLA in Schiermonnikoog using Sentinel-2 data?

Answers: Among studied multivariate models in this study, ANN using all 11 studied VIs as input with 5 as the number of hidden layers and Levenberg-Marquardt as training algorithm obtained the highest correlation between measured and predicted SLA values. The RMSE and R^2 were 0.47, 0.55 respectively. This finding shows that there is a non-linear correlation between SLA and spectral information of Sentinel-2 data in saltmarsh/wetland ecosystem due to field situation.

6.3.   Recommendations for further exploration

- Using higher number of samples in an appropriate time because using more sample data help to apply other training techniques and see the performance of the same statistical models.

- Using the equipment with higher precision to measure plant parameters, the equipment was not available to transfer to field; therefore, the area of leaves has been manually calculated.

- Exploring other multivariate models such as Random Forest (RF) and Support Vector Machines (SVMs) and comparing the results with studied multivariate models (ANN, and PLSR) in this research. To see using other multivariate models will improve the accuracy of SLA estimation in wetland ecosystems.

- Examining different satellite imageries such as Landsat 8 to estimate SLA in saltmarsh/ wetland ecosystem.

7.   APPENDICES

7.1.   Appendix I

The summary statistics between calculated Leaf Dry Matter Content (ratio of leaf dry mass to leaf fresh mass) in Schiermonnikoog island have been displayed in Table 7.1.

Table 7.1. The descriptive statistics for Leaf Dry Matter Content (ratio of leaf dry mass to leaf fresh mass) in Schiermonnikoog island (n=50).

Parameters	Leaf Dry Matter Content (LDMC)
Mean	0.30
Maximum	0.41
Minimum	0.13
Standard Deviation	0.06
Range	0.28
Coefficient of variation	0.2

7.2.   Appendix II

The Pearson's correlations between LDMC (ratio of leaf dry mass to leaf fresh mass) and the different measured plant parameters have been shown in Table 7.2

Table 7.2. The Pearson's correlation coefficient (r) between LA, SLA, and LDMC (ratio of leaf dry mass to leaf fresh mass)

Parameters	SLA (cm²/g)	Leaf Area (LA) (cm²)	Leaf Dry Matter Content (LDMC)
SLA	1		
LA	0.17	1	
LDMC	-0.66*	0.33	1

* $P \leq 0.05$

7.3. Appendix III

The correlations between the measured SLA and the predicted SLA through all 11 studied VIs using different regression models have been illustrated in Table 7.3.

Table 7.3. The correlation between measured and predicted SLA using studied VIs through different statistical regression models in Schiermonikoog isalnd based on validation set (n=20)

BAND/VI	LINEAR		QUADRATIC		LOGARITHMIC		EXPONENTIAL	
	R²	**RMSE**	**R²**	**RMSE**	**R²**	**RMSE**	**R²**	**RMSE**
SARVI2	0.31	0.74	0.19	0.96	-0.12	0.54	0.24	0.62
NMDI	0.11	0.68	0.09	0.54	0.05	0.51	0.11	0.76
SLAVI	0.15	0.76	0.11	0.65	0.17	0.56	0.14	0.66
VARI	0.13	0.67	0.13	0.73	0.16	0.69	0.26	0.62
SAVI	0.24	0.69	0.08	0.61	0.22	0.73	0.26	0.71
RVI	**0.46**	**0.64**	**0.40**	**0.65**	**0.42**	**0.66**	**0.38**	**0.67**
NDVI	0.24	0.65	0.08	0.58	0.22	0.71	0.26	0.76
GNDVI	0.17	0.66	0.34	0.62	0.09	0.64	0.18	0.64
NDMI	0.15	0.84	0.18	0.72	0.11	0.78	0.12	0.66
CAI	0.21	0.75	0.12	0.74	0.13	0.64	0.18	0.65
SWIRGVI	0.23	0.78	0.2	0.81	0.13	0.69	0.26	0.66

7.4.   Appendix IV

The map of the predicted SLA values using RVI has been displayed in Figure 7.1.
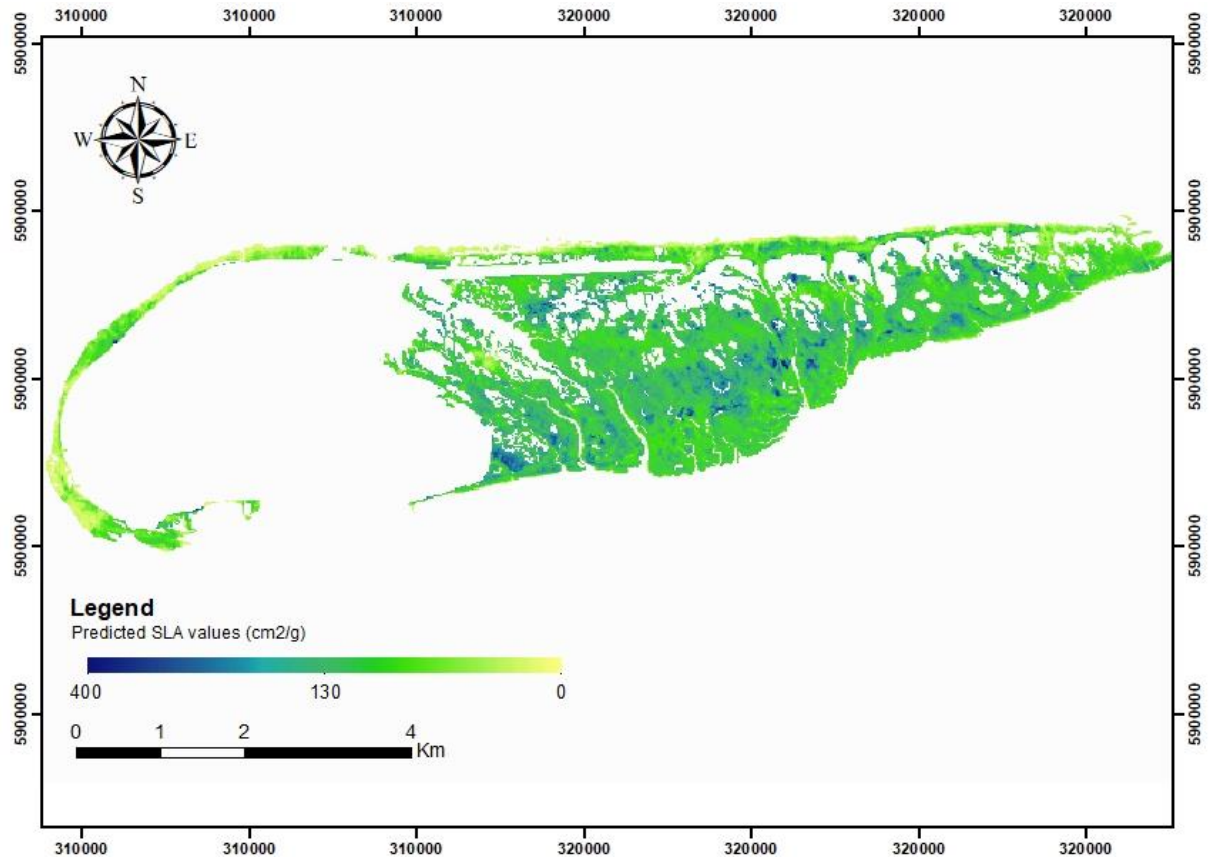
Figure 7.1. The map of modelled SLA in Scheirmonnikoog island using Senitnel-2B image on 15th September via RVI.

7.5.   Appendix V

The map of the predicted SLA values by the neural network (5 hidden layers, all 11 studied VIs as input, LM as training algorithm) has been displayed in Figure 7.2.
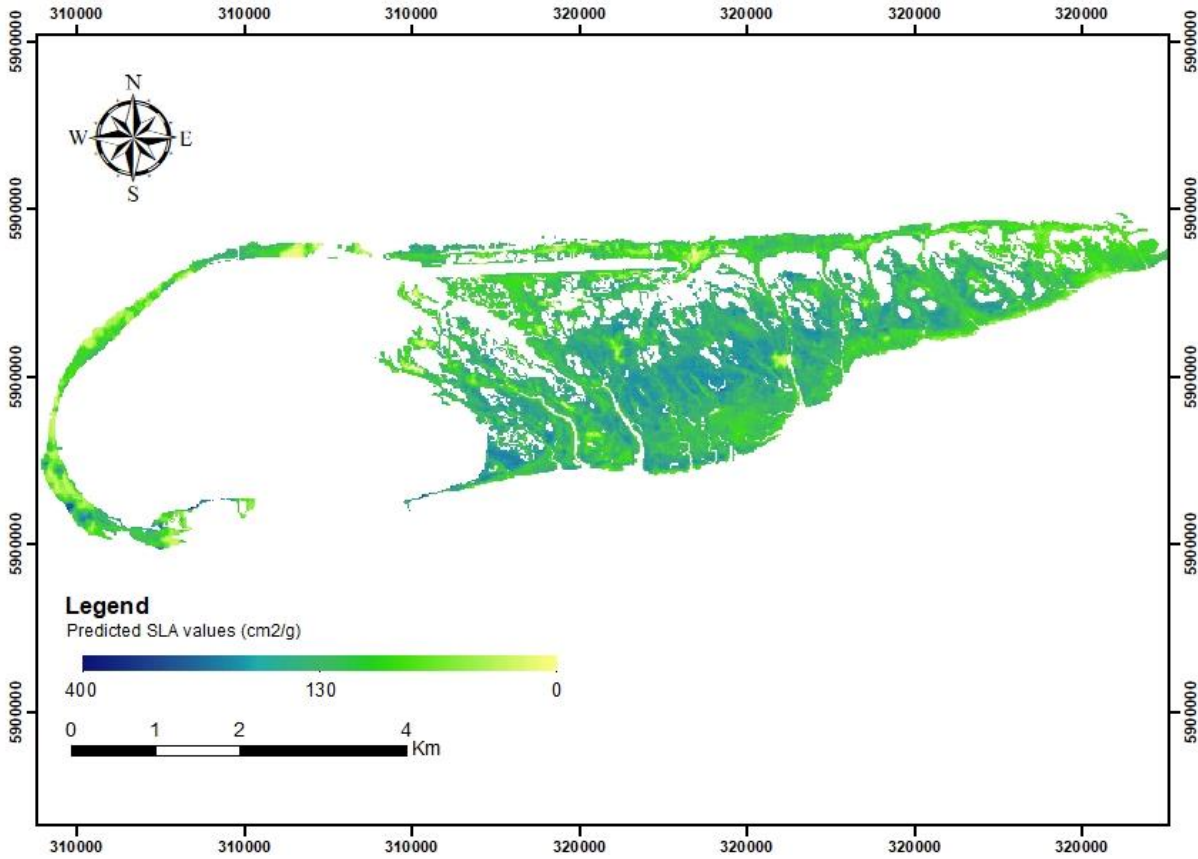

Figure 7.2. The map of modelled SLA in Scheirmonnikoog island using Senitnel-2B image on 15th September via ANN (5 hidden layers, all 11 studied VIs as input, LM as training algorithm).

LIST OF REFERENCES

Abdi, H., 2003. Partial Least Squares (PLS) Regression. Encycl. Res. methods Soc. Sci. 792–795. https://doi.org/http://dx.doi.org/10.4135/9781412950589.n690

Ackerly, D.D., Knight, C.A., Weiss, S.B., Barton, K., Starmer, K.P., 2002. Leaf size, specific leaf area and microhabitat distribution of chaparral woody plants: Contrasting patterns in species level and community level analyses. Oecologia 130, 449–457. https://doi.org/10.1007/s004420100805

Adam, E., Mutanga, O., Rugege, D., 2010. Multispectral and hyperspectral remote sensing for identification and mapping of wetland vegetation: A review. Wetl. Ecol. Manag. 18, 281–296. https://doi.org/10.1007/s11273-009-9169-z

Ali, A.M., 2016. Quantitative remote sensing of forest leaf functional traits. https://doi.org/10.3990/1.9789036542098

Ali, A.M., Darvishzadeh, R., Skidmore, A.K., 2017a. Retrieval of Specific Leaf Area From Landsat-8 Surface Reflectance Data Using Statistical and Physical Models. IEEE J. Sel. Top. Appl. Earth Obs. Remote Sens. 1–8. https://doi.org/10.1109/JSTARS.2017.2690623

Ali, A.M., Darvishzadeh, R., Skidmore, A.K., 2017b. Retrieval of Specific Leaf Area From Landsat-8 Surface Reflectance Data Using Statistical and Physical Models. IEEE J. Sel. Top. Appl. Earth Obs. Remote Sens. https://doi.org/10.1109/JSTARS.2017.2690623

Ali, A.M., Darvishzadeh, R., Skidmore, A.K., Duren, I. van, 2016a. Effects of Canopy Structural Variables on Retrieval of Leaf Dry Matter Content and Specific Leaf Area From Remotely Sensed Data. IEEE J. Sel. Top. Appl. Earth Obs. Remote Sens. 9, 898–909. https://doi.org/10.1109/JSTARS.2015.2450762

Ali, A.M., Darvishzadeh, R., Skidmore, A.K., Duren, I. Van, 2016b. Effects of Canopy Structural Variables on Retrieval of Leaf Dry Matter Content and Specific Leaf Area from Remotely Sensed Data. IEEE J. Sel. Top. Appl. Earth Obs. Remote Sens. 9, 898–909. https://doi.org/10.1109/JSTARS.2015.2450762

Ali, A.M., Darvishzadeh, R., Skidmore, A.K., Duren, I. van, Heiden, U., Heurich, M., 2016c. Estimating leaf functional traits by inversion of PROSPECT: Assessing leaf dry matter content and specific leaf area in mixed mountainous forest. Int. J. Appl. Earth Obs. Geoinf. 45, 66–76. https://doi.org/10.1016/j.jag.2015.11.004

Ali, A.M., Darvishzadeh, R., Skidmore, A.K., van Duren, I., 2017c. Specific leaf area estimation from leaf and canopy reflectance through optimization and validation of vegetation indices. Agric. For. Meteorol. 236, 162–174. https://doi.org/10.1016/j.agrformet.2017.01.015

Ali, A.M., Skidmore, A.K., Darvishzadeh, R., van Duren, I., Holzwarth, S., Mueller, J., 2016d. Retrieval of forest leaf functional traits from HySpex imagery using radiative transfer models and continuous wavelet analysis. ISPRS J. Photogramm. Remote Sens. 122, 68–80. https://doi.org/10.1016/j.isprsjprs.2016.09.015

Amiri, F., Rashid, A., Shariff, B.M., 2010. Using Remote Sensing Data for Vegetation Cover Assessment in Semi-Arid Rangeland of Center Province of Iran. World Apllied Sci. J. 11, 1537–1546.

Asner, G., Martin, R., 2008. Spectral and chemical analysis of tropical forests: Scaling from leaf to canopy levels. Remote Sens. Environ. 112, 3958–3970.

Asner, G.P., 1998. Biophysical and biochemical sources of variability in canopy reflectance. Remote Sens. Environ. 64, 234–253. https://doi.org/10.1016/S0034-4257(98)00014-5

Asner, G.P., Jones, M.O., Martin, R.E., Knapp, D.E., Hughes, R.F., 2008. Remote sensing of native and invasive species in Hawaiian forests. Remote Sens. Environ. 112, 1912–1926. https://doi.org/10.1016/j.rse.2007.02.043

Asner, G.P., Martin, R.E., Ford, A.J., Metcalee, D.J., Liddell, M.J., 2009. Leaf chemical and spectral diversity in Australian tropical forests. Ecol. Appl. 19, 236–253. https://doi.org/10.1890/08-0023.1

Asner, G.P., Martin, R.E., Tupayachi, R., Emerson, R., Martinez, P., Sinca, F., Powell, G.V.N., Wright, S.J., Lugo, A.E., 2011. Taxonomy and remote sensing of leaf mass per area (LMA) in humid tropical forests. Ecol. Appl. 21, 85–98. https://doi.org/10.1890/09-1999.1

Atkinson, P.M., Tatnall, A.R.L., 1997. Introduction neural networks in remote sensing. Int. J. Remote Sens. 18, 699–709. https://doi.org/10.1080/014311697218700

Atzberger, C., 2004. Object-based retrieval of biophysical canopy variables using artificial neural nets and radiative transfer models. Remote Sens. Environ. 93, 53–67.

https://doi.org/10.1016/j.rse.2004.06.016

Bacour, C., Baret, F., Béal, D., Weiss, M., Pavageau, K., 2006. Neural network estimation of LAI, fAPAR, fCover and LAI×Cab, from top of canopy MERIS reflectance data: Principles and validation. Remote Sens. Environ. 105, 313–325. https://doi.org/10.1016/j.rse.2006.07.014

Ball, A., Sanchez-Azofeifa, A., Portillo-Quintero, C., Rivard, B., Castro-Contreras, S., Fernandes, G., 2015a. Patterns of Leaf Biochemical and Structural Properties of Cerrado Life Forms: Implications for Remote Sensing. PLoS One 10, 1–15. https://doi.org/10.1371/journal.pone.0117659

Ball, A., Sanchez-Azofeifa, A., Portillo-Quintero, C., Rivard, B., Castro-Contreras, S., Fernandes, G., 2015b. Patterns of leaf biochemical and structural properties of Cerrado life forms: Implications for remote sensing. PLoS One 10, 1–15. https://doi.org/10.1371/journal.pone.0117659

Banskota, A., 2006. Estimating leaf area index of salt marsh vegetation using airborne hyperspectral data Estimating leaf area index of salt marsh vegetation using airborne hyperspectral data. Geo-Information Sci.

Baret, F., Guyot, G., 1991. Potentials and limits of vegetation indices for LAI and APAR assessment. Remote Sens. Environ. 35, 161–173. https://doi.org/10.1016/0034-4257(91)90009-U

Benediktsson, J.A., Sveinsson, J.R., Ersoy, O.K., Swain, P.H., 1993. Parallel consensual neural networks. IEEE Int. Conf. Neural Networks - Conf. Proc. 1993–Janua, 27–32. https://doi.org/10.1109/ICNN.1993.298536

Bourquin, J., Schmidli, H., Hoogevest, P. Van, Leuenberger, H., 1998. Technique for Data Sets Showing Non-Linear Relationships Using Data From a 7, 5–16.

Bowker, D.E., Davis, R.E., Myrick, D.L., Stacy, K., Jones, W.T., 1985. Spectral reflectances of natural targets for use in remote sensing studies. Hampton.

Carrascal, L.M., Galván, I., Gordo, O., 2009. Partial least squares regression as an alternative to current regression methods used in ecology. Oikos 118, 681–690. https://doi.org/10.1111/j.1600-0706.2008.16881.x

Chang, D., 2000. Estimation of Soil Physical Properties Using Remote Sensing and Artificial Neural Network. Remote Sens. Environ. 74, 534–544. https://doi.org/10.1016/S0034-4257(00)00144-9

Chen, K.S., Yen, S.K., Tsay, D.W., 1997. Neural classification of SPOT imagery through integration of intensity and fractal information. Int. J. Remote Sens. 18, 763–783. https://doi.org/10.1080/014311697218746

Chen, P., Jing, Q., 2017. A comparison of two adaptive multivariate analysis methods (PLSR and ANN) for winter wheat yield forecasting using Landsat-8 OLI images. Adv. Sp. Res. 59, 987–995. https://doi.org/10.1016/j.asr.2016.11.029

Cho, M.A., Skidmore, A., Corsi, F., van Wieren, S.E., Sobhan, I., 2007. Estimation of green grass/herb biomass from airborne hyperspectral imagery using spectral indices and partial least squares regression. Int. J. Appl. Earth Obs. Geoinf. 9, 414–424. https://doi.org/10.1016/j.jag.2007.02.001

Clevers, J.G.P.W., Kooistra, L., van den Brande, M.M.M., 2017. Using Sentinel-2 data for retrieving LAI and leaf and canopy chlorophyll content of a potato crop. Remote Sens. 9, 1–15. https://doi.org/10.3390/rs9050405

Corbane, C., Alleaume, S., Deshayes, M., 2013. Mapping natural habitats using remote sensing and sparse partial least square discriminant analysis. Int. J. Remote Sens. 34, 7625–7647. https://doi.org/10.1080/01431161.2013.822603

Cornelissen, J.H.C., Lavorel, S., Garnier, E., Díaz, S., Buchmann, N., Gurvich, D.E., Reich, P.B., Steege, H. ter, Morgan, H.D., Heijden, M.G.A. van der, Pausas, J.G., Poorter, H., 2003. A handbook of protocols for standardised and easy measurement of plant functional traits worldwide. Aust. J. Bot. 51, 335. https://doi.org/10.1071/BT02124

Curran, P.J., Dungan, J.L., Peterson, D.L., 2001. Estimating the foliar biochemical concentration of leaves with reflectance spectrometry: Testing the Kokaly and Clark methodologies. Remote Sens. Environ. 76, 349–359. https://doi.org/10.1016/S0034-4257(01)00182-1

Darvishzadeh, R., 2008a. Hyperspectral remote sensing of vegetation parameters using statistical and physical models. Geoinf. Sci.

Darvishzadeh, R., 2008b. Hyperspectral remote sensing of vegetation parameters using statistical and physical models. Geoinf. Sci. Wageningen.

Darvishzadeh, R., Atzberger, C., Skidmore, A. K., Schlerf, M., 2011. Mapping grassland leaf area index with airborne hyperspectral imagery: A comparison study of statistical approaches and inversion of

radiative transfer models. ISPRS J. Photogramm. Remote Sens. 66, 894–906. https://doi.org/10.1016/j.isprsjprs.2011.09.013

Darvishzadeh, R., Atzberger, C., Skidmore, A.K., Abkar, A.A., 2009. Leaf Area Index derivation from hyperspectral vegetation indicesand the red edge position. Int. J. Remote Sens. 30, 6199–6218. https://doi.org/10.1080/01431160902842342

Darvishzadeh, R., Skidmore, A. K., Schlerf, M., Atzberger, C., 2008. Inversion of a radiative transfer model for estimating vegetation LAI and chlorophyll in a heterogeneous grassland. Remote Sens. Environ. 112, 2592–2604. https://doi.org/10.1016/j.rse.2007.12.003

De Roeck, E.R., Verhoest, N.E.C., Miya, M.H., Lievens, H., Batelaan, O., Thomas, A., Brendonck, L., 2008. Remote sensing and wetland ecology: A South African case study. Sensors 8, 3542–3556. https://doi.org/10.3390/s8053542

Demuth, H., Hudson Beale, M., Hagan, M., 2017. Neural Network Toolbox ™ 6 User ' s Guide, Neural Network Toolbox™ 11 User's Guide. https://doi.org/10.1068/a4512 T4 - Thinking beyond ethnicity M4 - Citavi

Dorigo, W., Richter, R., Baret, F., Bamler, R., Wagner, W., 2009. Enhanced automated canopy characterization from hyperspectral data by a novel two step radiative transfer model inversion approach. Remote Sens. 1, 1139–1170. https://doi.org/10.3390/rs1041139

Drusch, M., Del Bello, U., Carlier, S., Colin, O., Fernandez, V., Gascon, F., Hoersch, B., Isola, C., Laberinti, P., Martimort, P., Meygret, A., Spoto, F., Sy, O., Marchese, F., Bargellini, P., 2012. Sentinel-2: ESA's Optical High-Resolution Mission for GMES Operational Services. Remote Sens. Environ. 120, 25–36. https://doi.org/10.1016/j.rse.2011.11.026

Du Plessis, W.P., 1999. Linear regression relationships between NDVI, vegetation and rainfall in Etosha National Park, Namibia. J. Arid Environ. 42, 235–260. https://doi.org/10.1006/jare.1999.0505

Duro, D.C., Coops, N.C., Wulder, M. a., Han, T., 2007. Development of a large area biodiversity monitoring system driven by remote sensing. Prog. Phys. Geogr. 31, 235–260. https://doi.org/10.1177/0309133307079054

Evans, J.R., 1989. Photosynthesis and nitrogen relationship in leaves of C3 plants. Oecologia 78, 9–19. https://doi.org/10.1007/BF00377192

Fang, H.L., Liang, S.L., 2003. Retrieving leaf area index with a neural network method: Simulation and validation. Geosci. Remote Sensing, IEEE Trans. 41, 2052–2062. https://doi.org/10.1109/TGRS.2003.813493

Fang, S., Le, Y., Liang, Q., Liu, X., 2014. Leaf Area Index Estimation Using Time-Series MODIS Data in Different Types of Vegetation. J. Indian Soc. Remote Sens. 42, 733–743. https://doi.org/10.1007/s12524-013-0349-1

Farifteh, J., Van der Meer, F., Atzberger, C., Carranza, E.J.M., 2007. Quantitative analysis of salt-affected soil reflectance spectra: A comparison of two adaptive methods (PLSR and ANN). Remote Sens. Environ. 110, 59–78. https://doi.org/10.1016/j.rse.2007.02.005

Fernández-manso, A., Fernández-manso, O., Quintano, C., 2016. International Journal of Applied Earth Observation and Geoinformation SENTINEL-2A red-edge spectral indices suitability for discriminating burn severity. Int. J. Appl. Earth Obs. Geoinf. 50, 170–175. https://doi.org/10.1016/j.jag.2016.03.005

Filella, I., Penuelas, J., 1994. The red edge position and shape as indicators of plant chlorophyll content, biomass and hydric status. Int. J. Remote Sens. 15, 1459–1470. https://doi.org/10.1080/01431169408954177

Foley, W.J., McIlwee, a, Lawler, I., Aragones, L., Woolnough, a P., Berding, N., 1998. Ecological applications of near infrared reflectance spectroscopy a tool for rapid, cost-effective prediction of the composition of plant and animal tissues and aspects of animal performance. Oecologia 116, 293–305. https://doi.org/10.1007/s004420050591

Fortuna, L., Rizzotto, G., Lavorgna, M., 2001. Pseudotumor cerebri, 1st ed, Neurologic Clinics. Springer-Verlag Londo. https://doi.org/10.1016/S0733-8619(03)00096-3

Foster, A.J., Kakani, V.G., Mosali, J., 2017. Estimation of bioenergy crop yield and N status by hyperspectral canopy reflectance and partial least square regression. Precis. Agric. 18, 192–209. https://doi.org/10.1007/s11119-016-9455-8

Gardner, M.., Dorling, S.., 1998. Artificial neural networks (the multilayer perceptron)—a review of applications in the atmospheric sciences. Atmos. Environ. 32, 2627–2636.

https://doi.org/10.1016/S1352-2310(97)00447-0

Geladi, P., Kowalski, B.R., 1986. Partial least-squares regression: a tutorial. Anal. Chim. Acta 185, 1–17. https://doi.org/10.1016/0003-2670(86)80028-9

Gitelson, A.A., Kaufman, Y.J., Merzlyak, M.N., 1996. Use of a green channel in remote sensing of global vegetation from EOS-MODIS. Remote Sens. Environ. 58, 289–298. https://doi.org/10.1016/S0034-4257(96)00072-7

Gitelson, A.A., Kaufman, Y.J., Stark, R., Rundquist, D., 2002. Novel algorithms for remote estimation of vegetation fraction. Remote Sens. Environ. 80, 76–87. https://doi.org/10.1016/S0034-4257(01)00289-9

Glossary of Neural Network Terms, 2018. Definition of Convergence (at Stand Out Publishing) - Netlab Loligo [WWW Document]. Stand Out Publ. URL http://standoutpublishing.com/g/convergence.html (accessed 3.12.18).

Goel, N.S., Strebel, D.E., 1983. Inversion of vegetation canopy reflectance models for estimating agronomic variables. I. Problem definition and initial results using the suits model. Remote Sens. Environ. 13, 487–507. https://doi.org/10.1016/0034-4257(83)90055-X

Grace, S., 2017. MODELLING AND MAPPING FOLIAR NITROGEN IN A WETLAND USING HIGH RESOLUTION IMAGES.

Haboudane, D., Miller, J.R., Pattey, E., Zarco-Tejada, P.J., Strachan, I.B., 2004. Hyperspectral vegetation indices and novel algorithms for predicting green LAI of crop canopies: Modeling and validation in the context of precision agriculture. Remote Sens. Environ. 90, 337–352. https://doi.org/10.1016/j.rse.2003.12.013

Hansen, P.M., Schjoerring, J.K., 2003. Reflectance measurement of canopy biomass and nitrogen status in wheat crops using normalized difference vegetation indices and partial least squares regression. Remote Sens. Environ. 86, 542–553. https://doi.org/10.1016/S0034-4257(03)00131-7

Hatfield, J.L., Gitelson, A.A., Schepers, J.S., Walthall, C.L., 2008. Application of spectral remote sensing for agronomic decisions. Agron. J. 100. https://doi.org/10.2134/agronj2006.0370c

Haykin, S., 1999. [Simon_Haykin]_Neural_Networks_A_Comprehensive_Fo(b-ok.org)book1.pdf, 2nd ed. ed. Prentice Hall International, Inc., Ontario.

Helland, I.S., 1988. On the structure of partial least squares regression. Commun. Stat. - Simul. Comput. 17, 581–607. https://doi.org/10.1080/03610918808812681

Hikosaka, K., 2004. Interspecific difference in the photosynthesis – nitrogen relationship : patterns , physiological causes , and ecological importance. Bot. Soc. Japan 117, 481–494. https://doi.org/10.1007/s10265-004-0174-2

Homolová, L., Malenovský, Z., Clevers, J.G.P.W., García-Santos, G., Schaepman, M.E., 2013a. Review of optical-based remote sensing for plant trait mapping. Ecol. Complex. 15, 1–16. https://doi.org/10.1016/j.ecocom.2013.06.003

Homolová, L., Malenovský, Z., Clevers, J.G.P.W., García-Santos, G., Schaepman, M.E., 2013b. Review of optical-based remote sensing for plant trait mapping. Ecol. Complex. 15, 1–16. https://doi.org/10.1016/j.ecocom.2013.06.003

Horler, D.N.H., Dockray, M., Barber, J., 1983. The red edge of plant leaf reflectance. Int. J. Remote Sens. 4, 273–288. https://doi.org/10.1080/01431168308948546

Hornik, K., Stinchcombe, M., White, H., 1989. Multilayer feedforward networks are universal approximators. Neural Networks 2, 359–366. https://doi.org/10.1016/0893-6080(89)90020-8

Hubert, M., Vanden Branden, K., 2003. Robust methods for partial least squares regression. J. Chemom. 17, 537–549. https://doi.org/10.1002/cem.822

Huete, A.R., 1988. A soil-adjusted vegetation index (SAVI). Remote Sens. Environ. 25, 295–309. https://doi.org/10.1016/0034-4257(88)90106-X

Huete, A.R., Liu, H.Q., Batchily, K., J., L. van W., 1997. A comparsion of vegetation indices over a Global set of TM images for EO -MODIS. Remote Sens. Environ. 59, 440–451.

Husbands, P., Jakobi, N., Smith, T., O'Shea, M., 1998. Better Living Through Chemistry: Evolving GasNets for Robot Control. Conn. Sci. 10, 185–210. https://doi.org/10.1080/095400998116404

Jiao, L., Pan, J., Fang, Y., 2001. Multiwavelet neural network and its approximation properties. IEEE Trans. Neural Networks 12, 1060–1066. https://doi.org/10.1109/72.950135

Jordan, C.F., Society, E., 1969. Derivation of Leaf-Area Index from Quality of Light on the Forest Floor Author (s): Carl F . Jordan Published by : Ecological Society of America Stable URL :

http://www.jstor.org/stable/1936256 . Ecology 50, 663–666. https://doi.org/10.2307/1936256

Klem, K., Ač, A., Holub, P., Kováč, D., Špunda, V., Robson, T.M., Urban, O., 2012. Interactive effects of PAR and UV radiation on the physiology, morphology and leaf optical properties of two barley varieties. Environ. Exp. Bot. 75, 52–64. https://doi.org/10.1016/j.envexpbot.2011.08.008

KNMI [WWW Document], 2018. URL http://www.knmi.nl/over-het-knmi/about (accessed 1.13.18).

Kohonen, T., 1988. An introduction to neural computing. Neural Networks 1, 3–16. https://doi.org/10.1016/0893-6080(88)90020-2

Kooistra, L., Salas, E.A.L., Clevers, J.G.P.W., Wehrens, R., Leuven, R.S.E.W., Nienhuis, P.H., Buydens, L.M.C., 2004. Exploring field vegetation reflectance as an indicator of soil contamination in river floodplains. Environ. Pollut. 127, 281–290. https://doi.org/10.1016/S0269-7491(03)00266-5

Korhonen, L., Hadi, Packalen, P., Rautiainen, M., 2017. Comparison of Sentinel-2 and Landsat 8 in the estimation of boreal forest canopy cover and leaf area index. Remote Sens. Environ. 195, 259–274. https://doi.org/10.1016/j.rse.2017.03.021

Lavorel, S., Grigulis, K., Lamarque, P., Colace, M.P., Garden, D., Girel, J., Pellet, G., Douzet, R., 2011. Using plant functional traits to understand the landscape distribution of multiple ecosystem services. J. Ecol. 99, 135–147. https://doi.org/10.1111/j.1365-2745.2010.01753.x

Lawrence, S., Giles, C.L., Tsoi, A.C., 1997. Lessons in neural network training: overfitting may be harder than expected. 14th Natl. Conf. Artificial Intell. 540–545.

Li, G., Lu, D., Moran, E., Hetrick, S., 2011. Land-cover classification in a moist tropical region of Brazil with Landsat TM imagery. Int. J. Remote Sensing2 32, 8207–8230. https://doi.org/10.1080/01431161.2010.532831.Land-cover

Li, W., Niu, Z., Chen, H., Li, D., 2016. Characterizing canopy structural complexity for the estimation of maize LAI based on ALS data and UAV stereo images. Int. J. Remote Sens. 38, 2106–2116. https://doi.org/10.1080/01431161.2016.1235300

Li, X., Zhang, Y., Bao, Y., Luo, J., Jin, X., Xu, X., Song, X., Yang, G., 2014. Exploring the best hyperspectral features for LAI estimation using partial least squares regression. Remote Sens. 6, 6221–6241. https://doi.org/10.3390/rs6076221

Liang, S., 2004. Quantitative Remote Sensing of Land Surfaces, 1st ed, Wiley Series on Remote Sensing. John Wiley Kr Sons, Inc, New Jersey. https://doi.org/10.1002/047172372X

Li, Wang, J., Tang, H., Huang, C., Yang, F., Chen, B., Wang, X., Xin, X., Ge, Y., 2016. Predicting grassland leaf area index in the meadow steppes of Northern China: A comparative study of regression approaches and hybrid geostatistical methods. Remote Sens. 8. https://doi.org/10.3390/rs8080632

Liu, M., Wang, Z., Li, S., Lü, X., Wang, X., Han, X., 2017. Changes in specific leaf area of dominant plants in temperate grasslands along a 2500-km transect in northern China. Sci. Rep. 7, 1–9. https://doi.org/10.1038/s41598-017-11133-z

Liu, P., Shi, R., Zhang, C., Zeng, Y., 2017. Integrating multiple vegetation indices via an artificial neural network model for estimating the leaf chlorophyll content of Spartina alterniflora under interspecies competition.

Lobell, D.B., Asner, G.P., Law, B.E., Treuhaft, R.N., 2001. Subpixel canopy cover estimation of coniferous forests in Oregon using SWIR imaging spectrometry. J. Geophys. Res. Atmos. 106, 5151–5160. https://doi.org/10.1029/2000JD900739

Lu, S., Lu, F., You, W., Wang, Z., Liu, Y., Omasa, K., 2018. A robust vegetation index for remotely assessing chlorophyll content of dorsiventral leaves across several species in different seasons. Plant Methods 14, 15. https://doi.org/10.1186/s13007-018-0281-z

Lymburner, L., Beggs, P., Jacobson, C., 2000. Estimation of canopy-average surface-specific leaf area using Landsat TM data. Photogramm. Eng. Remote Sens. 66, 183–191.

McCoy-Sulentic, M.E., Kolb, T.E., Merritt, D.M., Palmquist, E.C., Ralston, B.E., Sarr, D.A., 2017. Variation in species-level plant functional traits over wetland indicator status categories. Ecol. Evol. 7, 3732–3744. https://doi.org/10.1002/ece3.2975

Mcculloch, W.S., Pitts, W., 1990. a Logical Calculus of the Ideas Immanent in Nervous Activity. Bull. Mothemnticnl Biol. 52, 99–115. https://doi.org/10.1007/BF02478259

Messier, W.F., 1991. Artificial Neural Networks : Foundations and Application to a Decision Problem 3, 135–141.

Mirzaie, M., Darvishzadeh, R., Shakiba, A., Matkan, A.A., Atzberger, C., Skidmore, A., 2014. Comparative

analysis of different uni- and multi-variate methods for estimation of vegetation water content using hyper-spectral measurements. Int. J. Appl. Earth Obs. Geoinf. 26, 1–11. https://doi.org/10.1016/j.jag.2013.04.004

Monitoring, T., 2017. A Global Analysis of Sentinel-2A , Sentinel-2B and Landsat-8 Data Revisit Intervals and Implications for Terrestrial Monitoring. Remote Sens. 7, 1482–1503. https://doi.org/10.3390/rs9090902

Mulatu, H., 2006. Land covers change detection using Expert System and Hyperspectral imagery in the Islands of Schiermonnikoog, the Netherlands.

Multilayer Neural Network Architecture - MATLAB [WWW Document], 2018. . Mathworks. URL https://nl.mathworks.com/help/nnet/ug/multilayer-neural-network-architecture.html?requestedDomain=true (accessed 3.13.18).

Myneni, R.B., 1997. Estimation of global leaf area index and absorbed par using radiative transfer models. IEEE Trans. Geosci. Remote Sens. 35, 1380–1393. https://doi.org/10.1109/36.649788

Nagler, P.L., Inoue, Y., Glenn, E.P., Russ, A.L., Daughtry, C.S.T., 2003. Cellulose absorption index (CAI) to quantify mixed soil-plant litter scenes. Remote Sens. Environ. 87, 310–325. https://doi.org/10.1016/j.rse.2003.06.001

Nowlan, S.J., Hinton, G.E., 1992. Simplifying Neural Networks by Soft Weight-Sharing. Neural Comput. https://doi.org/10.1162/neco.1992.4.4.473

Paruelo, J.M., Tomasel, F., 1997. Prediction of functional characteristics of ecosystems: A comparison of artificial neural networks and regression models. Ecol. Modell. 98, 173–186. https://doi.org/10.1016/S0304-3800(96)01913-8

Pereira, H.M., Ferrier, S., Walters, M., Geller, G.N., Jongman, R.H.G., Scholes, R.J., Bruford, M.W., Brummitt, N., Butchart, S.H.M., Cardoso, A.C., Coops, N.C., Dulloo, E., Faith, D.P., Freyhof, J., Gregory, R.D., Heip, C., Höft, R., Hurtt, G., Jetz, W., Karp, D.S., McGeoch, M.A., Obura, D., Onoda, Y., Pettorelli, N., Reyers, B., Sayre, R., Scharlemann, J.P.W., Stuart, S.N., Turak, E., Walpole, M., Wegmann, M., 2013. Essential Biodiversity Variables. Science (80-.). 339, 277–278. https://doi.org/10.1126/science.1229931

Pierce, L., Running, S.W., Walker, J., 1994. Regional-scale relationships of leaf area index to specific leaf area and leaf nitrogen content. Ecol. Appl. 4, 313–321. https://doi.org/10.2307/1941936

Piotrowski, A.P., Napiorkowski, J.J., 2013. A comparison of methods to avoid overfitting in neural networks training in the case of catchment runoff modelling. J. Hydrol. 476, 97–111. https://doi.org/10.1016/j.jhydrol.2012.10.019

Poorter, H., Jong, R.O.B.D.E., 1999. A comparison of speci c leaf area, chemical composition and leaf construction costs of eld plants from 15 habitats di ering in productivity. October 143, 163–176.

Quan, X., He, B., Li, X., 2015. A Bayesian Network-Based Method to Alleviate the Ill-Posed Inverse Problem: A Case Study on Leaf Area Index and Canopy Water Content Retrieval. IEEE Trans. Geosci. Remote Sens. 53, 6507–6517. https://doi.org/10.1109/TGRS.2015.2442999

Reich, P.B., Ellsworth, D.S., Walters, M.B., 1998. Leaf structure (specific leaf area) modulates photosynthesis – nitrogen relations : evidence from within and across species and functional groups. Funct. Ecol. 12, 948–958. https://doi.org/10.1046/j.1365-2435.1998.00274.x

Riedmiller, M., Braun, H., 1993. A direct adaptive method for faster backpropagation learning: The RPROP algorithm. IEEE Int. Conf. Neural Networks - Conf. Proc. 1993–Janua, 586–591. https://doi.org/10.1109/ICNN.1993.298623

Rogers, K., 2012. Scientific modeling [WWW Document]. Encycl. Br. inc. URL https://www.britannica.com/science/scientific-modeling (accessed 1.27.18).

Rouse, J. W., J., Haas, R.H., Schell, J.A., Deering, D.W., 1974. Monitoring Vegetation Systems in the Great Plains with Erts, in: Stanley, C.F., Mercanti, E.P., Becker, M.A. (Eds.), Monitoring Vegetation Systems in the Great Plains with Erts. NASA, Washington, D.C., p. 309. https://doi.org/1974NASSP.351..309R

Rumelhart, D.E., Hinton, G.E., Williams, R.J. (1986), 1985. Learning internal representations by error propagation, in: Parallel Distributed Processing: Explorations in the Microstructure of Cognition, eds. MIT Press 1, 34.

Sánchez-Azofeifa, G.A., Castro, K., Wright, S.J., Gamon, J., Kalacska, M., Rivard, B., Schnitzer, S.A., Feng, J.L., 2009. Differences in leaf traits, leaf internal structure, and spectral reflectance between two communities of lianas and trees: Implications for remote sensing in tropical environments.

Remote Sens. Environ. 113, 2076–2088. https://doi.org/10.1016/j.rse.2009.05.013

Schmidt, K.S., Skidmore, A. K., 2003. Spectral discrimination of vegetation types in a coastal wetland. Remote Sens. Environ. 85, 92–108. https://doi.org/10.1016/S0034-4257(02)00196-7

Schmidt, K.S., Skidmore, A. K., Kloosterman, E.H., van Oosten, H., Kumar, L., Janssen, J. a. M., 2004. Mapping Coastal Vegetation Using an Expert System and Hyperspectral Imagery. Photogramm. Eng. Remote Sens. 70, 703–715. https://doi.org/10.14358/PERS.70.6.703

Schowengerdt, R.A., 2012. Remote Sensing: Models and Methods for Image Processing, 3rd ed. ed, Journal of environmental management. Tucson, Arizona. https://doi.org/10.1016/j.jenvman.2011.10.007

Schrama, M., 2012. The assembly of a salt marsh ecosystem - The interplay of green and brown webs 93, 240. https://doi.org/10.1890/11-1102.1

Serpico, S.B., Bruzzone, L., Roli, F., 1996. An experimental comparison of neural and statistical non-parametric algorithms for supervised classification of remote sensing images. Pattern Recognit. Lett. 17, 1331–1341.

Siegmann, B., Jarmer, T., 2015. Comparison of different regression models and validation techniques for the assessment of wheat leaf area index from hyperspectral data. Int. J. Remote Sens. 36, 4519–4534. https://doi.org/10.1080/01431161.2015.1084438

Skidmore, A.K., Pettorelli, N., Coops, N.C., Geller, G., Hansen, M., Lucas, R., Muncher, C.A., O'Connor, B., Paganini, M., Pereira, H.M., Schaepman, M.E., Turner, W., Wang, T., Wegman, M., 2015. Environmental science: Agree on biodiversity metrics to track from space. Nature 523, 403–405. https://doi.org/10.1038/523403a

Skidmore, A. K., 2002. Environmental modelling with GIS and remote sensing. Taylor & Francis.

Skidmore, A.K., Turner, B.J., Brinkhof, W., Knowles, E., 1997. Performance of a Neural Network: Mapping Forests Using GIS and Remotely Sensed Data. Photogramm. Eng. Remote Sens. 63, 501–514.

Song, C., Dannenberg, M.P., Hwang, T., 2013. Optical remote sensing of terrestrial ecosystem primary productivity. Prog. Phys. Geogr. 37, 834–854. https://doi.org/10.1177/0309133313507944

Stone, M., 1974. Regression Models and Life-Tables Author (s): D . R . Cox Source : Journal of the Royal Statistical Society . Series B (Methodological), Vol . 34 , No . 2 Published by : Wiley for the Royal Statistical Society Stable URL : http://www.jstor.org/stable/. J. R. Stat. Soc. 36, 111–147.

Sunar Erbek, F., Özkan, C., Taberner, M., 2004. Comparison of maximum likelihood classification method with supervised artificial neural network algorithms for land use activities. Int. J. Remote Sens. 25, 1733–1748. https://doi.org/10.1080/0143116031000150077

The European Space Agency (ESA), 2017. Sen2Cor | STEP [WWW Document]. URL http://step.esa.int/main/third-party-plugins-2/sen2cor/ (accessed 12.12.17).

the Secretariat of the Ramsar Convention, 2015. Duinen Schiermonnikoog | Ramsar Sites Information Service [WWW Document]. URL https://rsis.ramsar.org/ris/2214 (accessed 8.12.17).

Tilman, D., 2001. Functional diversity. Encycl. Biodivers. https://doi.org/10.1016/B0-12-226865-2/00132-2

Tiwari, R.S., Arora, M.K., Kailash, T., 1999. Soft classification for sub-pixel land cover extraction. J. Indian Soc. Remote Sens. 27, 225–234. https://doi.org/10.1007/BF02990835

Tobias, R.D., 2003. An introduction to partial least squares regression, in: SAS Conference Proceedings: SAS Users Group International 20 (SUGI 20). Cary, North Crolina, pp. 2–5. https://doi.org/http://support.sas.com/techsup/technote/ts509.pdf

Ullah, S., Skidmore, A.K., Ramoelo, A., Groen, T.A., Naeem, M., Ali, A., 2014. Retrieval of leaf water content spanning the visible to thermal infrared spectra. ISPRS J. Photogramm. Remote Sens. 93, 56–64. https://doi.org/10.1016/j.isprsjprs.2014.04.005

Ushada, M., Murase, H., 2006. Identification of a Moss Growth System using an Artificial Neural Network Model. Biosyst. Eng. 94, 179–189. https://doi.org/10.1016/j.biosystemseng.2006.03.001

van der Werff, H., van der Meer, F., 2016. Sentinel-2A MSI and Landsat 8 OLI provide data continuity for geological remote sensing. Remote Sens. 8, 883. https://doi.org/10.3390/rs8110883

Van Wittenberghe, S., Verrelst, J., Rivera, J.P., Alonso, L., Moreno, J., Samson, R., 2014. Gaussian processes retrieval of leaf parameters from a multi-species reflectance, absorbance and fluorescence dataset. J. Photochem. Photobiol. B Biol. 134, 37–48. https://doi.org/10.1016/j.jphotobiol.2014.03.010

Vernescu, C., Ryser, P., 2009. Constraints on leaf structural traits in wetland plants. Am. J. Bot. 96, 1068–1074. https://doi.org/10.3732/ajb.0800312

Verrelst, J., M, J., Alonso, L., Delegido, J., Rivera, J.P., Camps-Valls, G., Moreno, J., 2012. Machine learning regression algorithms for biophysical parameter retrieval: Opportunities for Sentinel-2 and -3. Remote Sens. Environ. 118, 127–139. https://doi.org/10.1016/j.rse.2011.11.002

Vile, D., Garnier, É., Shipley, B., Laurent, G., Navas, M.L., Roumet, C., Lavorel, S., Díaz, S., Hodgson, J.G., Lloret, F., Midgley, G.F., Poorter, H., Rutherford, M.C., Wilson, P.J., Wright, I.J., 2005. Specific leaf area and dry matter content estimate thickness in laminar leaves. Ann. Bot. 96, 1129–1136. https://doi.org/10.1093/aob/mci264

Violle, C., Navas, M.L., Vile, D., Kazakou, E., Fortunel, C., Hummel, I., Garnier, E., 2007. Let the concept of trait be functional! Oikos 116, 882–892. https://doi.org/10.1111/j.2007.0030-1299.15559.x

Vrieling, A., Skidmore, A.K., Wang, T., Meroni, M., Ens, B.J., Oosterbeek, K., O'Connor, B., Darvishzadeh, R., Heurich, M., Shepherd, A., Paganini, M., 2017. Spatially detailed retrievals of spring phenology from single-season high-resolution image time series. Int. J. Appl. Earth Obs. Geoinf. 59, 19–30. https://doi.org/10.1016/j.jag.2017.02.021

Wang, L., Qu, J.J., 2007. NMDI: A normalized multi-band drought index for monitoring soil and vegetation moisture with satellite remote sensing. Geophys. Res. Lett. 34, 1–5. https://doi.org/10.1029/2007GL031021

Wang, Q., Blackburn, G.A., Onojeghuo, A.O., Dash, J., Zhou, L., Zhang, Y., Atkinson, P.M., 2017. Fusion of Landsat 8 OLI and Sentinel-2 MSI Data. IEEE Trans. Geosci. Remote Sens. 55, 3885–3899. https://doi.org/10.1109/TGRS.2017.2683444

Williams, P., Norris, K., 1987. Near Infrared Technology in the Agricultural and Food Industries, American Association of Cereal Chemists, Inc.

Wilson, P.J., Thompson, K., Hodgson, J.G., 1999. Specific leaf area and dry leaf matter content as alternative predictors of plant strategies. New Phytol. 143, 155–162. https://doi.org/10.1016/j.cub.2011.03.016

Wilson, P.J., THOMPSON, K., HODGSON, J.G., 1999. Specific leaf area and leaf dry matter content as alternative predictors of plant strategies. New Phytol. 143, 155–162. https://doi.org/10.1046/j.1469-8137.1999.00427.x

Wold, H., 1975. Soft Modeling by Latent Variables; the Nonlinear Iterative Partial Least Squares Approach. Perspect. Probab. Stat. Pap. Honour M. S. Bartlett 117–142.

Wold, S., Sjöström, M., Eriksson, L., 2001. PLS-regression: A basic tool of chemometrics. Chemom. Intell. Lab. Syst. 58, 109–130. https://doi.org/10.1016/S0169-7439(01)00155-1

Wolter, P.T., Townsend, P.A., Sturtevant, B.R., 2009. Estimation of forest structural parameters using 5 and 10??meter SPOT-5 satellite data. Remote Sens. Environ. 113, 2019–2036. https://doi.org/10.1016/j.rse.2009.05.009

Yang, S., Feng, Q., Liang, T., Liu, B., Zhang, W., Xie, H., 2018. Modeling grassland above-ground biomass based on artificial neural network and remote sensing in the Three-River Headwaters Region. Remote Sens. Environ. 204, 448–455. https://doi.org/10.1016/j.rse.2017.10.011

Ye, X., Sakai, K., Sasao, A., Asada, S. ichi, 2008. Potential of airborne hyperspectral imagery to estimate fruit yield in citrus. Chemom. Intell. Lab. Syst. 90, 132–144. https://doi.org/10.1016/j.chemolab.2007.09.002

Yi, Q., Jiapaer, G., Chen, J., Bao, A., Wang, F., 2014. Different units of measurement of carotenoids estimation in cotton using hyperspectral indices and partial least square regression. ISPRS J. Photogramm. Remote Sens. 91, 72–84. https://doi.org/10.1016/j.isprsjprs.2014.01.004

Yuan, H., Yang, G., Li, C., Wang, Y., Liu, J., Yu, H., Feng, H., Xu, B., Zhao, X., Yang, X., 2017. Retrieving soybean leaf area index from unmanned aerial vehicle hyperspectral remote sensing: Analysis of RF, ANN, and SVM regression models. Remote Sens. 9. https://doi.org/10.3390/rs9040309